



Private 5G Networks for Connected Industries

Deliverable D5.3

E2E Performance Measurements and Analysis



Co-funded by the Horizon 2020 programme
of the European Union in collaboration with Taiwan

Date of Delivery: 31.12.2022
Project Start Date: 01.10.2019

Duration: 39 Months

Document Information

Project Number: 861459

Project Name: Private 5G Networks for Connected Industries

Document Number: D5.3

Document Title: E2E Performance Measurements and Analysis

Editor: Nicola di Pietro (ATH)

Authors: CC Weng, Jen-Sheng Huang (ANI),
Daniele Munaretto, Marco Centenaro, Daniele Ronzani,
Nicola di Pietro (ATH),
Henrik Klessig, David Ginthör (BOSCH),
Mickael Maman (CEA),
Cheng-Yi Chien, Jiun-Cheng Huang, Yen Wu, Jen-Hau
Chan (CHT),
Sven Wittig (HHI),
Mingzoo Wu, PoYu Liao, Frank Chih-Wei Su (III),
Shuo-Peng Liang, Jack Shi-Jie Luo (ITRI),
Sergio Barbarossa (SAP).

Dissemination Level: Public

Contractual Date of Delivery: 31.12.2022

Work Package WP5

File Name: 861459-5G_CONNI-D5-
3_E2E_Performance_Measurements_and_Analysis_v1-1

Revision History

Version	Date	Comment
0.1	25.08.2022	First table of contents by ATH.
0.2	28.09.2022	First contributions to Section 2 by ATH and to Section 4 by BOSCH.
0.3	27.10.2022	Contributions to Section 3 by III, to Section 2, 3, 4 by BOSCH, and to Section 3 by ITRI.
0.4	23.11.2022	Contributions to Section 3 by III, to Section 3 and 4 by BOSCH, and to Section 3 by HHI, to Section 2, 3, and 4 by ITRI.
0.5	25.11.2022	Final major contributions by all partners to all sections. Main editorial adaptations and preparation for internal review.
0.6	05.12.2022	Additional content by ITRI (Section 2 and 4), inclusion of first round of internal reviewer comments.
0.7	12.12.2022	Minor modifications, inclusion of second round of internal reviewer comments, discussed at the last plenary meeting of the project.
0.8	19.12.2022	Final corrections.
1.0	20.12.2022	Final submitted version.
1.1	09.06.2023	Revised version, updated after reception of the final review report. Comments received by the reviewers are addressed here

Executive Summary

This report is the third deliverable associated with 5G CONNI's WP5. It covers the period between month 30 and 39 of the project's lifetime, which corresponds to the conclusions of the activities of all WP5's tasks: Task 5.1 "Realization of the selected use cases", Task 5.2 "Test and evaluation in real-world production environments", and Task 5.3 "E2E performance measurement and KPI analysis."

This document describes the finalization of the deployment of 5G CONNI's end-to-end trial network that interconnects both the European and Taiwanese manufacturing facilities, as a conclusion of the work planned and begun as detailed in the previous deliverables of this WP. In particular, this document contains a finalized and complete list of all the hardware and software equipment utilized across the testbeds; a detailed reporting of the remaining network integration and use case deployments within and across the two continental testbeds; a collection of gathered use case results, key performance indicators, and analyses thereupon.

Table of Contents

Document Information	2
Revision History	3
Executive Summary	4
Table of Contents	5
List of Figures.....	7
List of Tables.....	8
List of Acronyms.....	9
1 Introduction	12
1.1 Scope and Structure.....	12
2 Final Hardware and Software Setup.....	14
2.1 End Devices	14
2.1.1 European Side	14
2.1.2 Taiwanese Side.....	16
2.2 Radio Access Equipment	18
2.2.1 European Side	18
2.2.2 Taiwanese Side.....	20
2.3 Core Network and MEC Equipment.....	21
2.3.1 European Side	21
2.3.1.1 Core Network.....	22
2.3.1.2 Multi-access Edge Computing	23
2.3.2 Taiwanese Side.....	23
2.3.2.1 Core Network.....	23
2.3.2.2 Multi-access Edge Computing	23
3 Completion of System Integration.....	25
3.1 European System Integration	25
3.1.1 Network Integration	25
3.1.2 Robot Integration.....	26
3.1.2.1 Motion Planning.....	29
3.1.2.2 Object Classification	29
3.1.2.3 Intrusion Detection.....	29
3.1.2.4 Robot Monitoring	29
3.1.2.5 Motion Control Logic and Motion Generator	29
3.1.3 Task List.....	30
3.1.3.1 Phase 1	30
3.1.3.2 Phase 2	30
3.2 Taiwanese System Integration	31

3.2.1	Network Integration	31
3.2.2	Task List.....	33
3.3	End-to-end System Integration	33
3.3.1	Final Architecture	33
3.3.2	5GC Unified Provisioning System Implementation	34
3.3.3	Task List.....	39
3.4	Timeline of the Task Lists.....	39
4	Final Performance Measurements and Analysis.....	41
4.1	European Testbed.....	41
4.1.1	Network.....	41
4.1.2	UC-3: Robot Platform with Edge Intelligence and Control	41
4.1.2.1	Workflow of Robot	41
4.1.2.2	Performance Evaluation	48
4.2	Taiwanese Testbed.....	55
4.2.1	Combined UC-1/UC-2: Process Diagnosis Using Augmented/Virtual Reality with CNC and Sensing Data Collection	55
4.2.1.1	Wired Performance Evaluation Using Network Emulator	55
4.2.1.2	Integration of 5G with Process Diagnosis Using AR/VR.....	58
4.2.2	Additional UC: Cloud-based Controller for Fixture System	59
4.2.2.1	Integration of 5G with Cloud-based Controller	59
4.3	End-to-end Testbed.....	60
4.3.1	Inter-site UC: Remote Expert Support for Process Diagnosis, Extension of UC-2 by Exchanging Data Across the Two Continental Sites	60
4.3.2	End Devices on BOSCH's Side.....	61
5	Conclusions.....	65
6	References.....	67

List of Figures

Figure 2-1: O-RAN rack, integrating core network and MEC equipment for the EU factory...	22
Figure 3-1: High-level structure of the EU multi-site 5G network.....	25
Figure 3-2: Main components of UC-3 setup.	27
Figure 3-3: Robot unit with 5G UE and NUC1 running the MS.....	28
Figure 3-4: Motion Application (MA) and Motion Service (MS) overview.....	28
Figure 3-5: Network architecture of remote testing.	32
Figure 3-6: EU-TW joint setup.	34
Figure 3-7: Legend of the architectural components of the EU-TW joint setup (in parentheses, the physical locations of each item).....	34
Figure 3-8: Centralized OAM for distributed 5GS management.	35
Figure 3-9: Remote access mechanism.	35
Figure 3-10: RESTful APIs for remote configuration and management.....	35
Figure 3-11: OAM UI.	37
Figure 3-12: Access management UI.	37
Figure 3-13: Session management UI.	38
Figure 3-14: SMF selection UI.	38
Figure 3-15: Graphical representation of WP5's implementation, integration, testing, and validation activities in the period covered by this deliverable.	40
Figure 4-1: Downlink network throughput.	41
Figure 4-2: Robot setup for sorting application.	42
Figure 4-3: Robot picking item up (left) and moving it in front of the camera (right).	43
Figure 4-4: Workflow of robot.	43
Figure 4-5: Output of motion planning tool.....	44
Figure 4-6: BOSCH Dinion Camera with video analytic connected over 5G router (left) and detection areas for intrusion alerts around the robot (right).....	45
Figure 4-7: Trajectory monitoring in Grafana.	46
Figure 4-8: Network monitoring in Grafana.	47
Figure 4-9: Setup for network performance evaluation of UC-3.	48
Figure 4-10: Frame rate and data rate of control packets between MA and MS.	49
Figure 4-11: DL latency of motion control frames with 0Mbps DL cross-traffic.....	50
Figure 4-12: Transfer-interval time measured after MA (left) and before MS (right) with 0Mbps DL cross-traffic.....	50
Figure 4-13: DL latency of motion control frames with 20Mbps DL cross-traffic.....	51
Figure 4-14: Transfer-interval time measured after MA (left) and before MS (right) with 20Mbps DL cross-traffic.....	51
Figure 4-15: DL latency of motion control frames with 150Mbps DL cross-traffic.....	52
Figure 4-16: Transfer-interval time measured after MA (left) and before MS (right) with 150Mbps DL cross-traffic.....	52
Figure 4-17: UL latency of motion control frames with no UL cross-traffic.....	52
Figure 4-18: Deviation from cycle time of motion control packets with 0, 20, and 150 Mbps DL cross-traffic.	53
Figure 4-19: Speed of robot joint for 0Mbps (left) and 150Mbps (right) cross-traffic.....	54
Figure 4-20: Close-up view of speed of robot joint for 0Mbps (left) and 150Mbps (right) cross-traffic.	54
Figure 4-21: Deviation between commanded and executed trajectory speed for 0Mbps (left) and 150Mbps (right) cross-traffic.	54
Figure 4-22: Illustration of inter-site use case.	55
Figure 4-23: Network architecture of impairments emulation.	56
Figure 4-24: Throughput measurements of remote render over ideal transport network.	56

Figure 4-25: Snapshot of streaming video via remote render over ideal transport network. ...57
 Figure 4-26: Integration of 5G system with combined UC-1 and UC-2.....58
 Figure 4-27: Vibration mitigation using cloud-based controller over 5G.59
 Figure 4-28: Illustration of vibration mitigation.59
 Figure 4-29: Architecture of the inter-site use case.....60
 Figure 4-30: Virtual machine on 5G smartphone.62
 Figure 4-31: Virtual machine on tablet (left) with external 5G module (right).....62
 Figure 4-32: Downlink traffic for machine visualization as data rate (left) and frame rate (right).....63
 Figure 4-33: Uplink traffic for updating viewpoint as data rate (left) and frame rate (right). ...63
 Figure 4-34: Latency distribution for downlink (left) and uplink traffic (right).....64

List of Tables

Table 2-1: End devices at BOSCH's factory.14
 Table 2-2: 5G routers.15
 Table 2-3: End devices at BOSCH's factory for the inter-site UC.....16
 Table 2-4: End device at HHI.....16
 Table 2-5: CNC devices at TW side.....17
 Table 2-6: Cloud-based controller equipment at IMTC.....17
 Table 2-7: End-user connectivity devices at TW side.18
 Table 2-8: RAN equipment at BOSCH.....18
 Table 2-9: ANI RAN equipment at HHI.19
 Table 2-10: RAN equipment at ITRI.....20
 Table 2-11: 5GC equipment at BOSCH.....22
 Table 2-12: 5GC equipment at HHI.22
 Table 2-13: MEC equipment at BOSCH.23
 Table 2-14: 5GC equipment at ITRI.....23
 Table 2-15: MEC equipment at ITRI.24
 Table 3-1: Interoperability test items for ANI's gNB and ATH's UPF integration.....26
 Table 3-2: Task list for Phase 1.30
 Table 3-3: Task list for Phase 2.31
 Table 3-4: Interoperability test items.....32
 Table 3-5: Task list for in-lab and on-premises integration.....33
 Table 3-6: Task list for end-to-end integration.39
 Table 4-1: Remote render with simulated latency.57

List of Acronyms

3D	3-Dimensional
3GPP	3 rd Generation Partnership Project
5G	5 th Generation of mobile networks
5GC	5G Core network
5G CONNI	5G for Connected Industries
5QI	5G QoS Identifier
AF	Application Function
AMF	Access and Mobility management Function
ANI	Alpha Networks Inc. (partner of the consortium)
API	Application Programming Interface
AR	Augmented Reality
ATH	Athonet Srl (partner of the consortium)
AUSF	Authentication Server Function
AWS	Amazon Web Services
BOSCH	Robert Bosch GmbH (partner of the consortium)
CBC	Cloud-Based Control
CDF	Cumulative Distribution Function
CHT	Chunghwa Telecom Co. Ltd. (partner of the consortium)
CNC	Computer Numerical Control
CP	Control Plane
CPE	Customer-Premises Equipment or Customer-Provided Equipment
CPU	Central Processing Unit
CU	Central Unit
DL	Downlink
DN	Data Network
DNN	Data Network Name
DU	Distributed Unit
DX.Y	Deliverable X.Y (where X and Y are numbers)
E2E	End-to-End
eMBB	enhanced Mobile Broad Band
EU	Europe/European
FCAPS	Fault-management, Configuration, Accounting, Performance and Security
gNB	gNodeB (5G base station using NR technology)
GPU	Graphics Processing Unit
GUI	Graphical User Interface
GUTI	Globally Unique Temporary ID
GW	Gateway
HHI	Fraunhofer Heinrich Hertz Institute (partner of the consortium)
HQ	Headquarters
HW	Hardware
II	Institute for Information Industry (partner of the consortium)
IMSI	International Mobile Subscriber Identity
IMTC	(ITRI's) Intelligent Machinery Technology Center

IP	Internet Protocol
ITRI	Industrial Technology Research Institute Inc. (partner of the consortium)
KPI	Key Performance Indicator
MA	Motion Application
MAC	Medium Access Control
MCS	Modulation and Coding Scheme
MEC	Multi-access Edge Computing
MIMO	Multiple-Input Multiple-Output
MQTT	Message Queue Telemetry Transport
MS	Motion Service
N/A	Not Applicable
NEF	Network Exposure Function
NF	Network Function
NG	Next Generation
NGAP	Next-Generation Application Protocol
NMS	Network Management Station
NR	New Radio
NRF	Network Repository Function
NUC	Next Unit of Computing
OAM	Operations, Administration, and Maintenance
ONVIF	Open Network Video Interface Forum
OP	OPerator code
OPC	Derived OPerator Code
OTT	Over-The-Top
O-RAN	Open Radio Access Network
PC	Personal Computer
PCF	Policy Control Function
PDCP	Packet Data Convergence Protocol
PDU	Protocol Data Unit
PHY	Physical Layer
PoE	Power over Ethernet
PPTP	Point-to-Point Tunneling Protocol
PREEMPT RT	Preemptive Real Time
PTP	Precision Time Protocol
QoS	Quality of Service
RAM	Random-Access Memory
RAN	Radio Access Network
REST	REpresentational State Transfer
RF	Radio Frequency
RLC	Radio Link Control
RRC	Radio Resource Control
RU	Radio Unit
SA	Standalone
SCTP	Stream Control Transmission Protocol
SMF	Session Management Function

SSD	Solid State Drive
SW	Software
TCP	Transmission Control Protocol
TSN	Time-Sensitive Networking
TW	Taiwan/Taiwanese
UC	Use Case
UDM	Unified Data Management
UDP	User Datagram Protocol
UE	User Equipment
UI	User Interface
UL	Uplink
UP	User Plane
UPF	User Plane Function
URLLC	Ultra-Reliable and Low-Latency Communications
USB	Universal Serial Bus
UE	User Equipment
VPN	Virtual Private Network
VR	Virtual Reality
WP	Work Package
WPX	Work Package X (where X is a number)

1 Introduction

This deliverable formally concludes the activities of 5G CONNI's WP5 on "Integration, Demonstration & Verification." Overall, WP5's scope was to build an end-to-end (E2E) trial deployment that implements and validates the innovative networking and use-case-supporting solutions that were the object of 5G CONNI's work.

[1] and [2] treated:

- the testbeds' architectural design, specifically chosen by the consortium partners for the project's use cases (UCs) in the first part of the WP's work;
- the practical aspects of the components' integration into a coherent E2E setup;
- and the initial in-lab integration and testing.

The main outcomes of such work can be summarized as follows:

- The architectural framework of the E2E demonstration, designed to support an extension of the Augmented/Virtual Reality for Process Diagnosis UC (cf. [3] and [4]).
- An initial identification of the required hardware (HW) and software (SW) equipment.
- The formalization of an integration roadmap with well-defined intermediate integration tasks, conceived to efficiently lead the consortium step by step towards the full deployment of the networks and UC infrastructure that now support the European (EU) and Taiwanese (TW) setups.
- A description of the testing tools and procedures utilized along the intermediate integration steps and the initial available test results.

The present deliverable is conceived as the straightforward consequence and prosecution of [1] and [2]. It describes the fully in-factory operational deployment reached at the end of the project's lifetime, and it includes all gathered functional and performance results. Although some information is recalled whenever opportune, we recommend that a reader is familiar with the content of [1] and [2] before reading this document.

1.1 Scope and Structure

This document was written with a very pragmatic perspective, and similarly to the previous deliverables of WP5, its intent is to report very concretely on the implementation and result collection aspects that characterize the project's demonstrational setups. It consolidates, completes, and partially updates the information contained in [1] and [2]. More precisely, this document:

- Provides a final and exhaustive catalogue of the HW and SW equipment involved in the testbed (cf. Section 2).
- Details the completion of the testbed integration activities carried out at the EU and TW sites between month 30 and 39 of the project's lifetime (cf. Section 3). In particular:
 - The deployment at HHI (EU site) of an edge node with User Plane Function (UPF)'s functionalities and of a new piece of Radio Access Network (RAN) equipment provided by ANI and pre-tested at ITRI's facilities (TW site) – see Section 3.1.1 and Section 3.2.1.
 - The full installation and feature description of the robot used for the UC at BOSCH's factory (EU side) – see Section 3.1.2.

- The completion of the development of the unified provisioning system that jointly manages the users and User Equipment (UE) data of both the EU and TW 5G network's sides (cf. Section 3.3.2).
- The full installation and configuration of over-the-top (OTT) applications for the deployed UCs.
- Contains the collection of the experimental results and key performance indicator (KPI) measurement from the implemented UCs (complemented also by the results already reported in [5]) – see Section 4.

Furthermore, as a reference and for coherence with what reported in [1] and [2], we include the list of all the intermediate tasks that have led to the full testbed integration and results collection (cf. Section 3.1.3, Section 3.2.2, and Section 3.3.3), and a graphical representation of their scheduling during the WP's progress (cf. Section 3.4).

2 Final Hardware and Software Setup

The following subsections provide the final and exhaustive component-by-component inventory and the technical specification of the HW and SW equipment involved and integrated in the EU and TW setups, updating and fully completing the content of Section 3 of [1] and [2], where this inventory was initiated. For a detailed description of the multi-site EU and TW architectural configuration and the role that each partner’s site plays in the intercontinental deployment, please refer to Section 2 of [1] and [2].

Section 2.1, 2.2, and 2.3 treat respectively:


1. End devices, consisting of both traditional UEs such as smartphones and tablets and robots/workstations integrated with Customer Premise Equipment (CPE).
2. Radio access equipment (two base stations deployed in the EU setup, one in the TW).
3. 5G Core network (5GC) and Multi-access Edge Computing (MEC) equipment at both EU and TW sides, plus an on-cloud 5GC instance.

2.1 End Devices

2.1.1 European Side

At the EU factory (BOSCH), as reported in [1], the robot is used for the demonstration of UC-3 (“Robot Platform with Edge Intelligence and Control,” cf. [3]). Additionally, further HW and SW components have been added during the development of the robot application. These include additional workstations and cameras as described in the following tables.


Table 2-1: End devices at BOSCH’s factory.


Hardware	Software
<p>Franka Emika Panda Robot</p> <ul style="list-style-type: none"> • 7-degrees-of-freedom robot arm for research purposes • Ethernet, TCP/IP and UDP/IP for real-time commands • Firmware 1.3.2 • Control sampling frequency: 1 kHz between controller and arm (to be extended by an edge cloud-based closed-loop control) 	<p>Franka Emika Panda Robot</p> <ul style="list-style-type: none"> • Libfranka 0.5.0 (C++ Library)
<p>Intel NUC</p> <ul style="list-style-type: none"> • Cloud controller operating the robot • 100BASE-TX network card (Intel I219-V) 	<ul style="list-style-type: none"> • Ubuntu 16.04 LTS Xenial Xerus and PREEMPT_RT_patched_kernel 4.14.78-rt47 • Motion planning framework MoveIt 2.2 based on ROS 2

	<ul style="list-style-type: none"> • ROS integration library for Franka Emika (https://github.com/frankaemika/franka_ros) • OpenCV 4.6.0 • Grafana 9.2.0 with InfluxDB 2.4
<p>Camera Vivotek IB8360</p> <ul style="list-style-type: none"> • Ethernet IP Camera • Ethernet 10/100Base-T(X) • 1080p 	
<p>Camera BOSCH DINION IP 8000</p> <ul style="list-style-type: none"> • Ethernet IP Camera • Ethernet 10/100Base-T(X) • 1080p 	<p>BOSCH Intelligent Video Analytics 8.10</p>

In [1], multiple UEs have been considered to provide wireless connectivity between the robot and the controller running on the workstation PC. In the final setup, we used the Robustel 5G Router which can provide simultaneous connectivity over 5G for the robot and the Vivotek Camera to the controller. The BOSCH camera is connected over a dedicated Milesight 5G router.

Table 2-2: 5G routers.

Hardware	Software
<p>Robustel R5020 Industrial 5G Router</p> <ul style="list-style-type: none"> • 5G 4 × 4 MIMO support • 4 x 1 GBase-T Ethernet 	<p>Robustel RobustOS R5020 Firmware V5.0.0</p>

<p>Milesight UR75 Industrial 5G Router</p> <ul style="list-style-type: none"> • 5G 4x4 MIMO support • 4 x 1 GBase-T Ethernet 	<p>UR75 Firmware v76.2.0.8</p>
--	--------------------------------

For the inter-site UC, which is an extension of UC-2 conducted on the TW side, additional HW and SW is used. This includes a workstation PC for the 3D rendering and two additional UEs to display the virtual machine.

Table 2-3: End devices at BOSCH's factory for the inter-site UC.

Hardware	Software
<p>Workstation PC</p> <ul style="list-style-type: none"> • CPU: Intel i7-11700K • GPU: RTX 3080 TI • 1GBase-T Ethernet 	<ul style="list-style-type: none"> • Windows Server 2022 Standard • SQLServer 2019 • Dassault Systèmes: 3DEXPERIENCE 2021X FD04 • SteamVR 1.17 • Nvidia CloudXR 3.2
<p>Samsung Galaxy Tab S7</p>	<p>Android 11</p>
<p>Quectel 5G RM500Q development board</p>	
<p>Asus Zenfone 8</p> <ul style="list-style-type: none"> • Qualcomm® Snapdragon™ 888 5G Mobile Platform 	<p>Android 11</p>
<p>Raspberry Pi 3 Model B</p> <ul style="list-style-type: none"> • ARM Cortex A53 4x 1,2GHz 	<p>Raspberry Pi OS Kernel Version 5.10.63</p>

On the other hand, at the EU enterprise’s headquarters (HQ), coinciding with HHI’s premises, a Linux Notebook equipped with an external USB 5G modem is used:

Table 2-4: End device at HHI.

Hardware	Software
<p>Quectel RM500Q-GL modem on RMU500-EK evaluation board</p>	<p>Linux</p>

2.1.2 Taiwanese Side

This section describes the end devices operating at the TW manufacturing site (ITRI). The (Computer Numerical Control) CNC cell used to demonstrate UC-1 (“Process diagnostics by CNC and Sensing Data collection”) and UC-2 (“Using AR/VR for process diagnosis”), described in [3], is as follows:

Table 2-5: CNC devices at TW side.

Hardware	Software
<p>CNC Machine Tool Travel</p> <ul style="list-style-type: none"> Multi-task machine tool with five axes X-Axis Travel mm 560 Y-Axis Travel mm ±125 Z-Axis Travel mm 560+93 W-Axis Travel mm 910 B-Axis Rotating Angle degree - 20°~200° C-Axis Rotating Angle degree 360° <p>CNC Data Collection for AR/VR and Analysis</p> <ul style="list-style-type: none"> Industrial PC Intel Celeron J1900, 4GB DDR3 LMemory GbE, 4XUSB 	<p>CNC Machine Tool Controller</p> <ul style="list-style-type: none"> Siemens 840D Solution Line with OPCUA data interface (OP67) and C# for data access (OP66) <p>CNC Data Collection for AR/VR and Analysis</p> <ul style="list-style-type: none"> Operating System: Windows 10 Embedded

The cloud-based controller of a fixture system (cf. the additional UCs proposed in [3], Section 2.5) that operates at the TW factory (IMTC) is described in the following table:

Table 2-6: Cloud-based controller equipment at IMTC.

Hardware	Software
<p>3X2 POGO ARRAY</p> <ul style="list-style-type: none"> Each POGO uses two motors to control 3-degrees-of-freedom for fixture purposes. Ethernet, TCP/IP for real-time commands. Control sampling frequency: 4kHz between controller and Servo Driver (to be extended by a Ground Controller-based closed-loop control) <p>Cloud Controller</p> <ul style="list-style-type: none"> Workstation with 1000BASE-TX network card (Intel I210) <p>Ground Controller</p> <ul style="list-style-type: none"> Workstation with 1000BASE-TX network card (Intel I210) 	<p>3X2 POGO ARRAY</p> <ul style="list-style-type: none"> L2100 motion controller 109.06.03 (C Library) <p>Cloud Controller</p> <ul style="list-style-type: none"> Windows Embedded Standard 7 Service Pack 1 32-bit operating systems <p>Ground Controller</p> <ul style="list-style-type: none"> Windows Embedded Standard 7E Service Pack 1 32-bit operating systems INTime version 5.2.14234, Patch level 14234

Finally, the CPEs that provide 5G connectivity to the appliances are described in the following table:

Table 2-7: End-user connectivity devices at TW side.

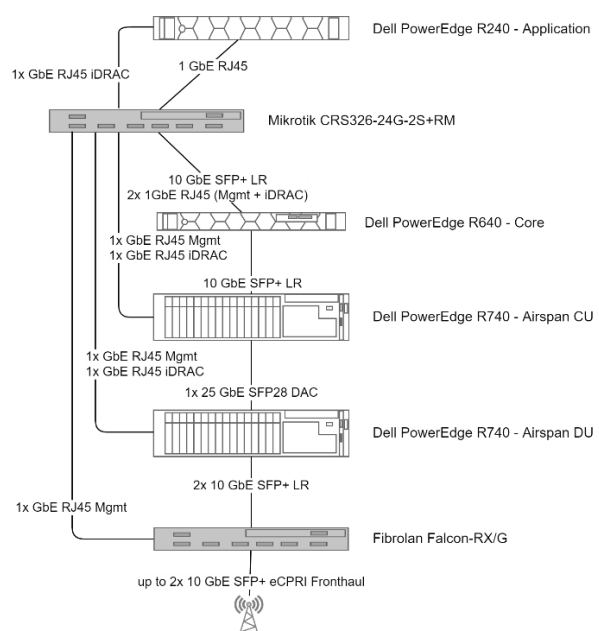
Hardware	Software
<p>5G NR CPE</p> <ul style="list-style-type: none"> 5G NR Sub-6: Base on Qualcomm SDX55 CPU: Qualcomm IPQ6010 WiFi: 802.11ax 2 x 2 Interfaces: <ul style="list-style-type: none"> 2 x LAN Ethernet-1GE WLAN (802.11ax) USB 2.0 Type A DIDO RS232C/RS485 Bluetooth 5.0 <p>5G dongle</p> <ul style="list-style-type: none"> Quanta WU7 <p>AR/VR user device</p> <ul style="list-style-type: none"> iPad Pro (2nd generation) 	<p>5G NR CPE</p> <ul style="list-style-type: none"> Operating System: Linux <p>AR App for Process diagnostics</p> <ul style="list-style-type: none"> Customized Hololens App developed with Unity3D/C# <p>VR App for remote expert</p> <ul style="list-style-type: none"> Customized App based-on Dassault Systèmes 3D Experience and 3D Excite developed with C#

2.2 Radio Access Equipment

2.2.1 European Side

The radio access equipment deployed at the EU factory (BOSCH's premises) is described in the following table:


Table 2-8: RAN equipment at BOSCH.

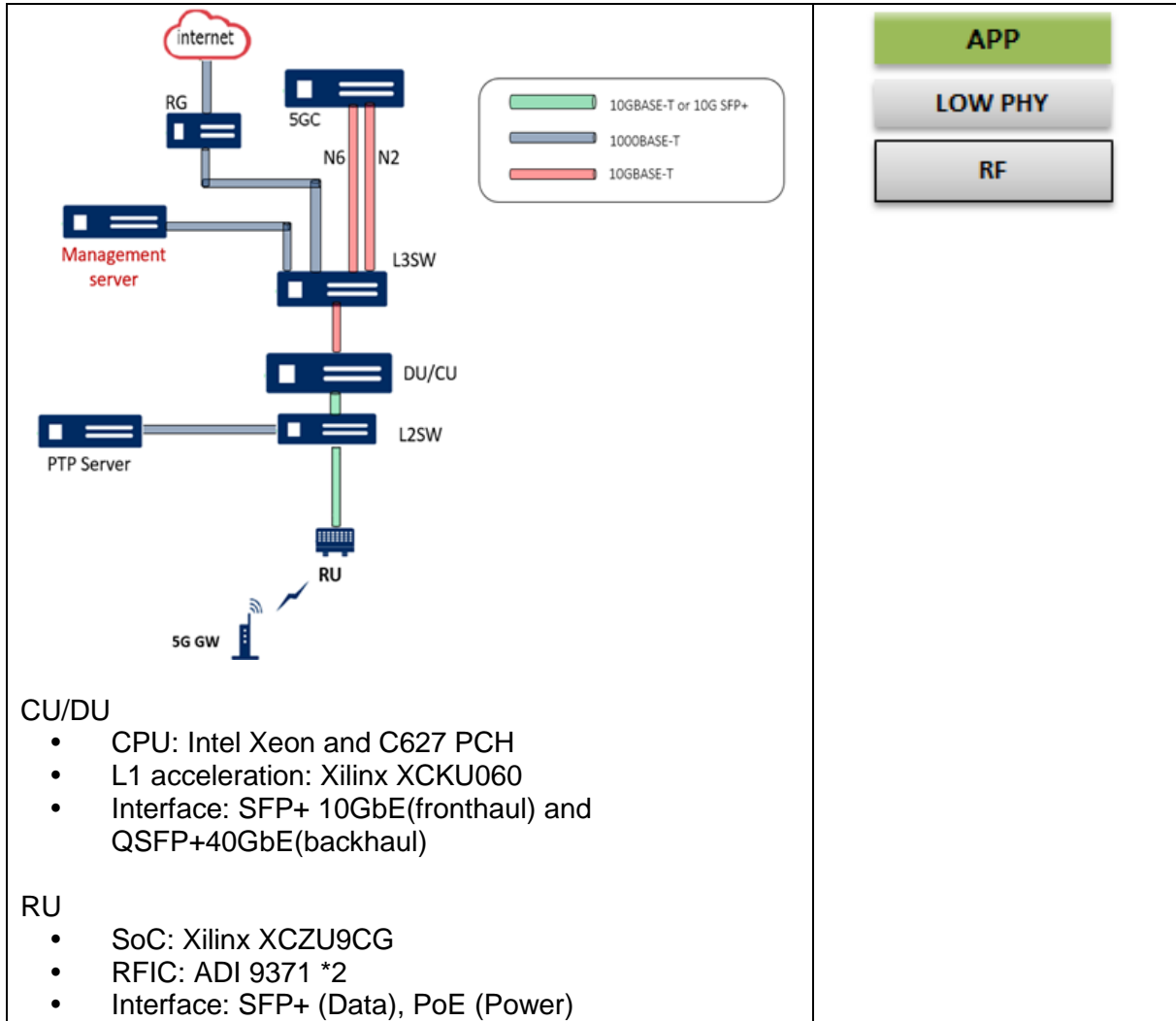
Hardware	Software																								
<p>Open-RAN (O-RAN) Rack Physical</p> 	<p>O-RAN Rack Virtual Machines</p> <table border="1" data-bbox="813 1276 1388 1904"> <tr> <td>VM k8s master</td> <td>VM k8s node Airspan CU</td> <td>VM Airspan NMS</td> <td>VM NMS DB - MSSQL</td> </tr> <tr> <td colspan="4">VMware ESXi 7.0</td> </tr> <tr> <td colspan="4">Dell PowerEdge R740</td> </tr> <tr> <td colspan="4">k8s node Airspan DU</td> </tr> <tr> <td colspan="4">CentOS 7</td> </tr> <tr> <td colspan="4">Dell PowerEdge R740</td> </tr> </table>	VM k8s master	VM k8s node Airspan CU	VM Airspan NMS	VM NMS DB - MSSQL	VMware ESXi 7.0				Dell PowerEdge R740				k8s node Airspan DU				CentOS 7				Dell PowerEdge R740			
VM k8s master	VM k8s node Airspan CU	VM Airspan NMS	VM NMS DB - MSSQL																						
VMware ESXi 7.0																									
Dell PowerEdge R740																									
k8s node Airspan DU																									
CentOS 7																									
Dell PowerEdge R740																									
<p>RAN CU Server: Dell PowerEdge R740</p> <ul style="list-style-type: none"> CPU: Intel® Xeon® Gold 5218R RAM: 160 GB SSD: 480 GB 	<p>Hypervisor:</p> <ul style="list-style-type: none"> VMware ESXi 7.0 <p>Operating System:</p> <ul style="list-style-type: none"> CentOS 7/8 																								

<ul style="list-style-type: none"> • 2 x Intel® XXV710 (4 x 25 GbE) • 1 x Intel® XL710 (2 x 40 GbE) • 4 x 1 GbE 	<p>Applications:</p> <ul style="list-style-type: none"> • Kubernetes Master • Airspan OpenRANGE vCU <ul style="list-style-type: none"> ◦ CP/UP Split Deployment via 3GPP E1 Interface • Airspan ACP (NMS) • MS-SQL Database
<p>RAN DU Server: Dell PowerEdge R740</p> <ul style="list-style-type: none"> • CPU: Intel® Xeon® Gold 5218R • RAM: 256 GB • SSD: 480 GB • 1 x Intel® XXV710 (2x 25 GbE) • 1 x Intel® XL710 (4x 10 GbE) • Accelerator card: Silicom Pomona Lake 	<p>Operating System:</p> <ul style="list-style-type: none"> • CentOS 7 <p>Applications:</p> <ul style="list-style-type: none"> • Airspan OpenRANGE vDU <ul style="list-style-type: none"> ◦ 3GPP Split 2 - F1 Interface towards CU ◦ RAN Split 7.2x towards RU
<p>Radio Unit: Airspan AirVelocity 2700</p> <ul style="list-style-type: none"> • NR Band n78 • 4T4R (4x 250 mW) • 100 MHz Bandwidth • SFP+ port • Synchronization: PTP, SyncE • Power: 48V DC, 50W 	<ul style="list-style-type: none"> • O-RAN Split 7.2a
<p>RAN Switch: Fibrolan Falcon RX/G</p> <ul style="list-style-type: none"> • 12 x SFP+ • 8 x SFP28 • PTP, SyncE w/ ITU G.8275.1 profile • GNSS Receiver • External Sync IO (1PPS/10 MHz) 	

As for the radio access equipment deployed at the EU enterprise’s HQ (HHI), it is provided by ANI to foster the international collaboration among the project’s partners. It is described in the following table:

Table 2-9: ANI RAN equipment at HHI.

Hardware	Software
RAN structure	<p>CU/DU</p>  <p>RU</p>

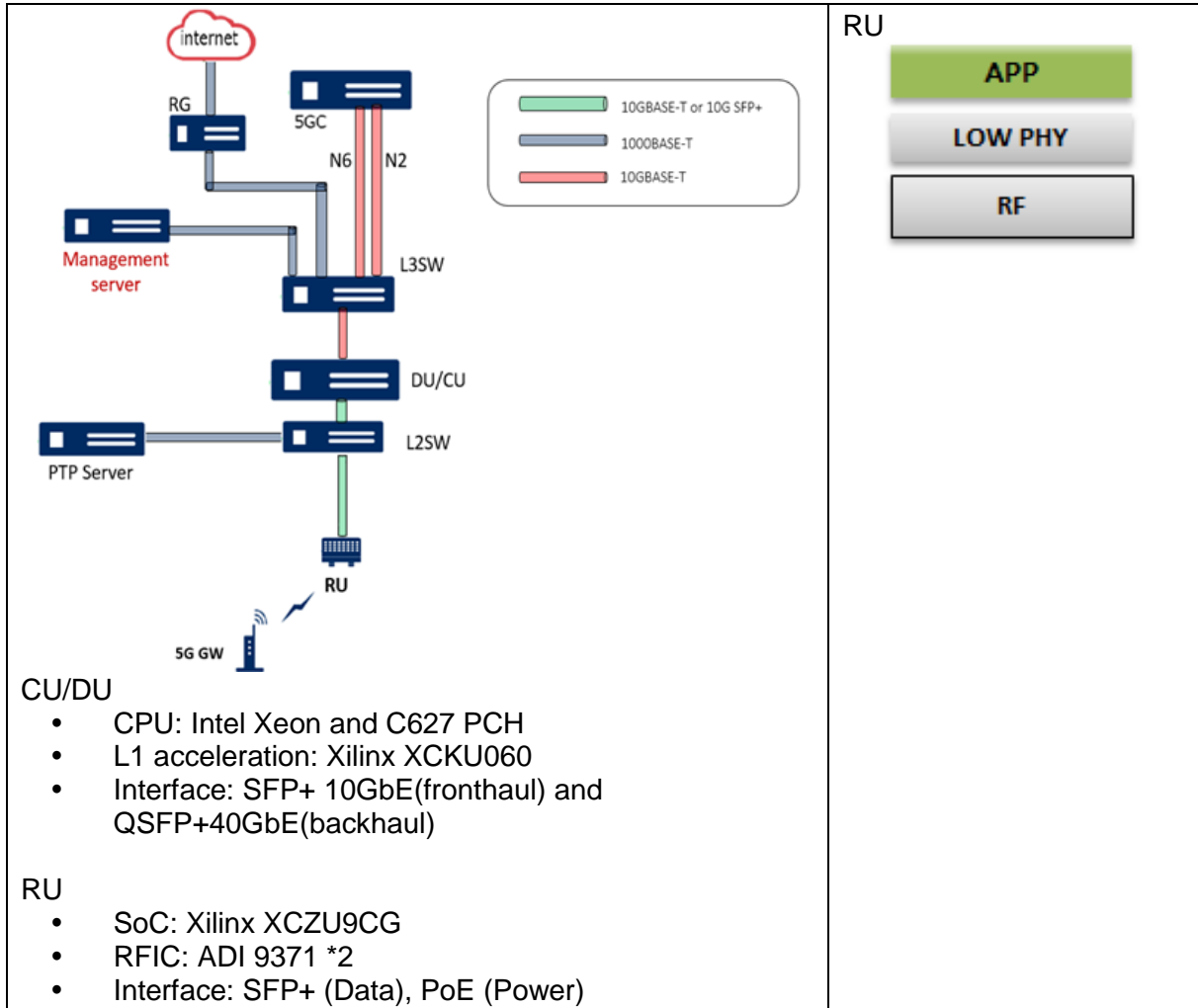


2.2.2 Taiwanese Side

The radio access equipment deployed at the TW manufacturing site is described in the following table:

Table 2-10: RAN equipment at ITRI.

Hardware	Software
RAN structure	<p>CU/DU</p> <p>RRC NGAP</p> <p>PDCP SCTP</p> <p>RLC</p> <p>MAC</p> <p>HIGH PHY</p> <p>BSP</p> <p>x86</p>



2.3 Core Network and MEC Equipment

2.3.1 European Side

As far as the EU factory environment is concerned, we highlight that the 5GC and MEC equipment embedded in the O-RAN rack will provide a full on-site solution comprising the mobile core and edge computing servers close to the RAN equipment. The following figure shows the detail of the O-RAN rack composition.

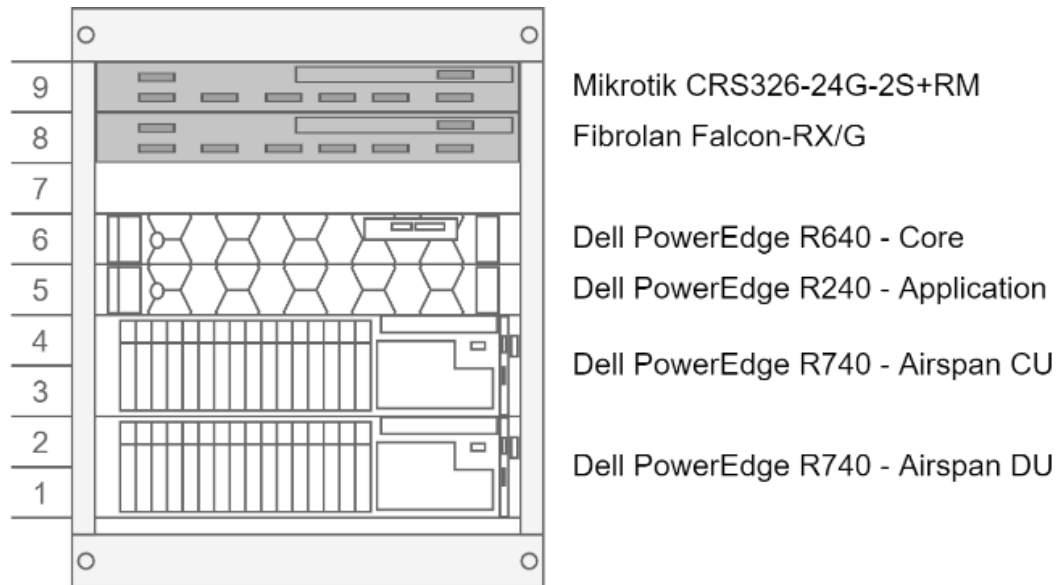


Figure 2-1: O-RAN rack, integrating core network and MEC equipment for the EU factory.

2.3.1.1 Core Network

The core network equipment deployed at the EU factory is described in the following table:

Table 2-11: 5GC equipment at BOSCH.

Hardware	Software
Dell R640: <ul style="list-style-type: none"> • Intel Xeon CPU Gold 6140 2.3G, 18C/36T • 128 GB RAM • 2 x 600 GB 15K rpm SAS 12Gbps (RAID 1) • 2 x 32 GB microSD (RAID 1) • 2 x Hot-plug, Redundant Power Supply (1+1), 750W • 2 x 10 GbE • 8 x 1 GbE 	VMs: <ul style="list-style-type: none"> • 5GC – Athonet’s Griffone Hypervisor: <ul style="list-style-type: none"> • VMware ESXi Operating System: <ul style="list-style-type: none"> • Linux Yocto

At the enterprise’s HQ (HHI), instead, the following 5GC edge node (UPF functionality) is deployed:

Table 2-12: 5GC equipment at HHI.

Hardware	Software
Dell PowerEdge R240: <ul style="list-style-type: none"> • CPU: Intel® Xeon® E2100 • RAM: 64 GB • 1 x Hot-plug, 250W • 2 x 1 GbE 	VMs: <ul style="list-style-type: none"> • UPF Hypervisor: <ul style="list-style-type: none"> • VMware ESXi Operating System: <ul style="list-style-type: none"> • Linux Yocto

Further, as described in more detail in Section 3.3.1.1 of [2], the EU on-site network deployments are interconnected via Virtual Private Network (VPN) with an on-cloud 5G control plane instance, running on AWS.

2.3.1.2 Multi-access Edge Computing

As said previously, the MEC equipment hosting the BOSCH Application Function (AF) is integrated in the O-RAN rack that will be deployed at the EU factory, and its specifications are as follows:

Table 2-13: MEC equipment at BOSCH.

Hardware	Software
Dell PowerEdge R240 <ul style="list-style-type: none"> • CPU: Intel® Xeon® E2134 • RAM: 16 GB • SSD: 1 TB • 2 x 1 GbE 	Hypervisor <ul style="list-style-type: none"> • VMware ESXi Edge cloud controller: <ul style="list-style-type: none"> • A state-of-the-art-based [6] Motion Application in the edge cloud (written in Python) controls the robot movements at a slightly higher cycle time than 1 ms [3] Extension of robot SW <ul style="list-style-type: none"> • Robot movements are interpolated and executed through a Franka Motion Service [6] (written in C++) • Franka Motion Service uses libfranka; see Section 3.1.1 of [1]

2.3.2 Taiwanese Side

2.3.2.1 Core Network

The 5GC equipment deployed at the TW data center is described in the following table:

Table 2-14: 5GC equipment at ITRI.

Hardware	Software
5GC Server: Dell PowerEdge R630 <ul style="list-style-type: none"> • CPU: Intel® Xeon® E5 2603 v4 • RAM: 128GB DDR4 up to 2400MT/s • DISK: 0.96TB hot-plug SATA SSD SmartNIC: Agilio CX 2 x 10GbE <ul style="list-style-type: none"> • Interfaces: 2-port 10GbE, SFP+ • Memory: 2GB DDR3 onboard memory 	5GC Software Platform: <ul style="list-style-type: none"> • Kubernetes Scheduler • Kubernetes API server 5GC Application: <ul style="list-style-type: none"> • AMF/SMF/AUSF/UDM/UPF Operating Systems: <ul style="list-style-type: none"> • Ubuntu Hypervisors: <ul style="list-style-type: none"> • Linux KVM

2.3.2.2 Multi-access Edge Computing

The MEC equipment deployed at the TW manufacturing site is described in the following table:

Table 2-15: MEC equipment at ITRI.

Hardware	Software
<p>Control Node Server: Dell R740xd</p> <ul style="list-style-type: none"> • CPU: 2*Intel® Xeon® Gold 6254, 3.10 GHz, 18cores • RAM: 256 GB • DISK: 1.2TB • NIC: 4* GE4 port (Intel Chip) <p>Compute Node: Dell R740xd</p> <ul style="list-style-type: none"> • CPU: 2*Intel® Xeon® Gold 6254, 3.10 GHz, 18cores • RAM: 256 GB • DISK: 1.2TB • NIC: 4* GE4 port (Intel Chip) • 4 port Intel Corporation Ethernet Controller X710 for 10GbE SFP+ • 4 port Intel Corporation I350 Gigabit Network Connection <p>SDN Switch Edge-Core 5812-54X-O-AC-F</p> <ul style="list-style-type: none"> • 48 SFP + support 10GbE (DAC, 10GBASE-SR / LR) or 1GbE (1000BASE-T / SX / LX) • PicOS 	<p>Platform:</p> <ul style="list-style-type: none"> • ECoreCloud MANO • Openstack Control • Openstack Compute <p>VNF:</p> <ul style="list-style-type: none"> • Mobile Edge Enabler Control Plane • Mobile Edge Enabler Data Processor

3 Completion of System Integration

In this section, we describe the activities that led to the conclusion of the integration of the EU and TW continental systems, comprising different physical sites, as per the architecture formalized in [1] and [2] and recalled in Section 3.3.1. Specifically, we report on the work carried out from the submission of [2] until the end of the project. As a reference, at the end of each of the following subsections, we also recall the lists of intermediate tasks carried out before, and that led to the completion of the integration activities, as defined in [1] and [2].

3.1 European System Integration

As reported in the following, the conclusion of the network integration activities at the EU side consisted of:

- the installation of a gNodeB (gNB) and an edge node with UPF functionalities at HHI,
- the corresponding interoperability tests,
- and the improvement of the 5G network performance at BOSCH.

After describing such activities, we move to a detailed report of the robot integration activities at BOSCH for the implementation of UC-3.

3.1.1 Network Integration

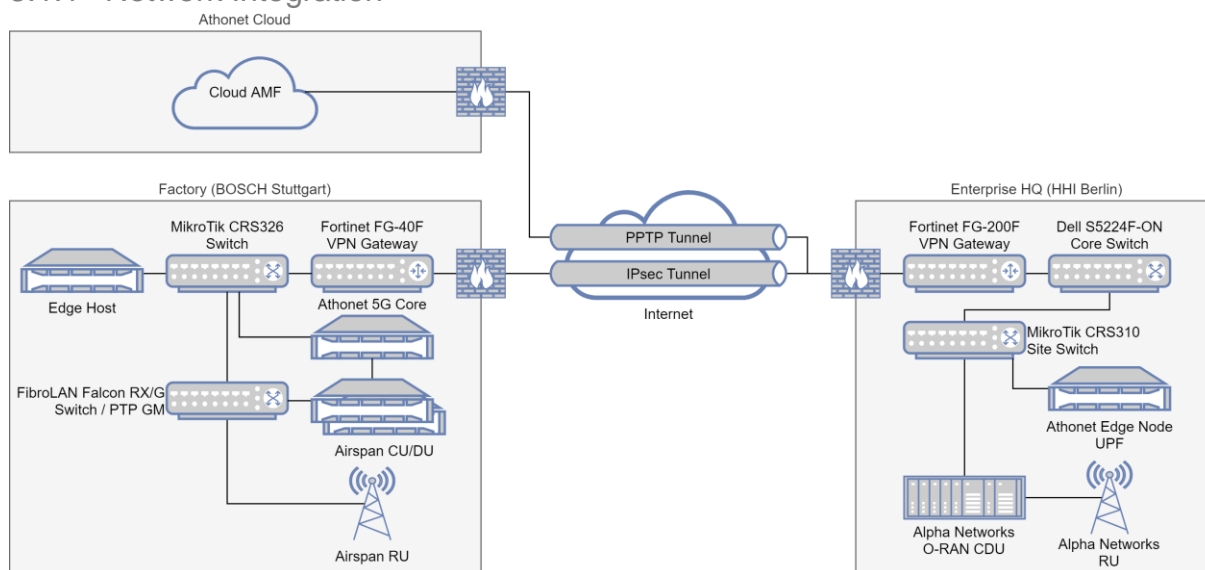


Figure 3-1: High-level structure of the EU multi-site 5G network.

As planned in [2] and recalled in Section 3.1.3.2, full Phase-2 network integration was completed, resulting in the network depicted in the high-level overview of Figure 3-1. Building on the Phase-1 fully private network defined in [2], the European 5G system was extended to include HHI's Berlin campus representing the enterprise's HQ. On this location, an O-RAN compliant gNB consisting of an integrated CU/DU and a separate RU, both supplied by ANI, and an edge server hosting the 5G's UPF for local traffic breakout supplied by ATH were integrated. The site is connected via a Point-to-Point Tunneling Protocol (PPTP) VPN connection to a cloud-hosted 5G control plane, thus implementing the *hybrid 5G network deployment model* (see [7]). For this network, user profiles are provisioned to the on-cloud control plane's Unified Data Management (UDM) via the common provision system developed for the 5G CONNI international network (see Section 3.3.2). Subsequently, the following

basic functional tests were performed to validate interoperability (the list of tests coincides with that of the in-lab integration activities reported in Section 3.2.1):

Table 3-1: Interoperability test items for ANI's gNB and ATH's UPF integration.

TEST ID	TITLE	Test Purpose	Result
1.1	NG Setup	Successful NG interface setup between gNB and 5GC	Pass
1.2	UE Initial Registration with IMSI identity	UE initial registration with IMSI identity	Pass
1.3	UE Initial Registration with GUTI identity	UE initial registration with GUTI identity	N/A
1.4	PDU Session Establishment	Successful establishment of the PDU session	Pass
1.5	Data Transfer using Ping application	Successful data transfer between the UE and external data network (e.g. 8.8.8.8)	N/A
1.6	UE Deregistration	Successful deregistration procedure triggered by the UE entering flight mode	Pass
1.7	Access Network Release	AN release due to user inactivity	Pass
1.8	UE-Triggered Service Request	Successful MO (Mobile Originated) Service Request	Pass

Notice that the scope of the gNB-5GC integration at HHI (simulated enterprise's HQ) was to demonstrate *functional* interoperability between ANI and ATH's components and did not include advanced KPI optimization activities. On the EU side, performance optimization was instead one of the goals of the in-factory 5G network deployment at BOSCH. In this case, a throughput performance of 153 Mbps (TCP DL) was already reported in [2]. This behavior was non-optimal and relatively low compared to our targets. This was caused by an interoperability issue between gNB and the 5GC's Session Management Function (SMF) related to the handling of Quality of Service (QoS) flows, which forced classification of all traffic as signaling traffic to be transmitted with a lower and more robust Modulation and Coding Scheme (MCS). After a successful root-cause analysis, the issue was fixed in a subsequent software release, leading to a significant throughput performance improvement (+ 87%). Performance measurements for the final configuration of the in-factory network are reported in Section 4.1.1.

3.1.2 Robot Integration

This section describes the complete setup of UC-3 in the BOSCH plant. The main goal of this UC is to demonstrate the wireless operation of a robot arm and the offloading of its control application to a central cloud.

The first in-lab integration took place in the BOSCH Renningen Campus and was reported in Section 4.1.3 of [2]. The key aspect in this report was the split of the robot control into the Motion Application (MA) and the Motion Service (MS). This split is a prerequisite to enable

real-time operation of the robot over a potentially unreliable and non-deterministic network. The robot has a hard requirement on the cycle time of 1 ms, which cannot be achieved by the Release-15 network used in the trial. The MA, which is located remotely behind the 5G network, can at most provide a cycle time in the range of 10 ms. To solve this issue, we introduced the MS, which is a lightweight application that runs directly at the robot. In its core, it has an interpolator function which receives the control data from the MA, removes jitter and interpolates it such that a constant and deterministic data stream with 1ms cycle time to the robot is guaranteed. The MA represents the actual controller which selects the motion trajectories and determines the correct control commands for the robot.

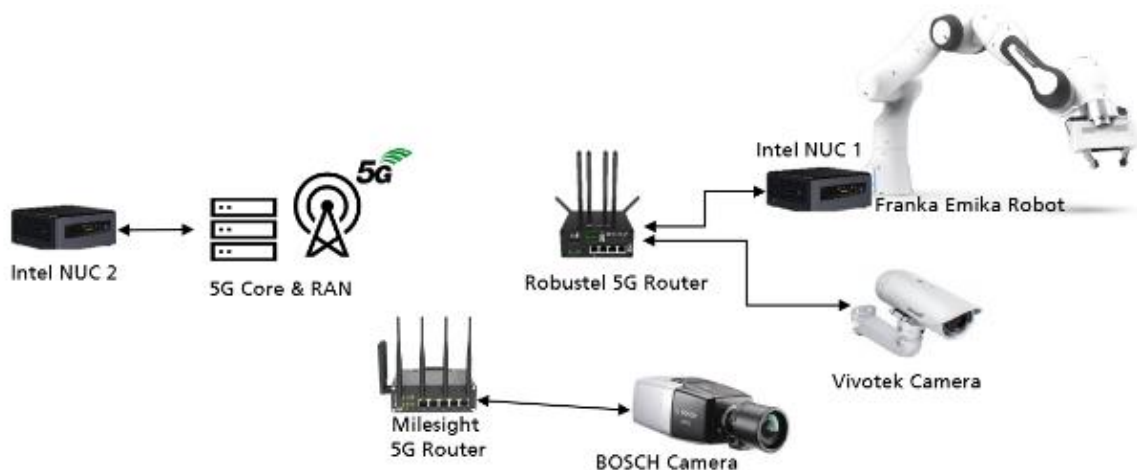


Figure 3-2: Main components of UC-3 setup.

While in [2] the MA only contained a basic motion generator based on a sine curve, we enhanced the motion application by further functionalities. The main application of the robot in the final setup is to perform a “pick & place” task, where items from a tray are sorted into two different containers. To execute the sorting application, several features were implemented, including:

- robot control split into MS and MA,
- motion planning for the pick & place operation,
- object classification for the sorting application,
- intrusion detection, and
- robot monitoring Graphical User Interface (GUI).

The main HW components of this UC are shown in Figure 3-2. The Franka robot and the Vivotek IP camera for object classification are operated wirelessly over 5G through the same Robustel 5G router. Figure 3-3 shows the robot with its control unit including the 5G UE and the NUC 1 running the MS. The Franka control box on the bottom converts the joint vectors transmitted by the NUC 1 to control signals to steer the servo drives of the robot. The only purpose of the network switch shown in the image is to provide Power over Ethernet (PoE) to the Vivotek Ethernet Camera. The robot controller running on NUC 2 and the Bosch Camera for intrusion detection, which is operated from a larger distance from the robot, are connected to the core-side of the 5G system. This setup allows for flexible deployment of the robot in different locations in the factory. The robot unit requires no rewiring and can be placed at any location with 5G connectivity and a power outlet. The detailed component description and software list is provided in Section 2.1.1.

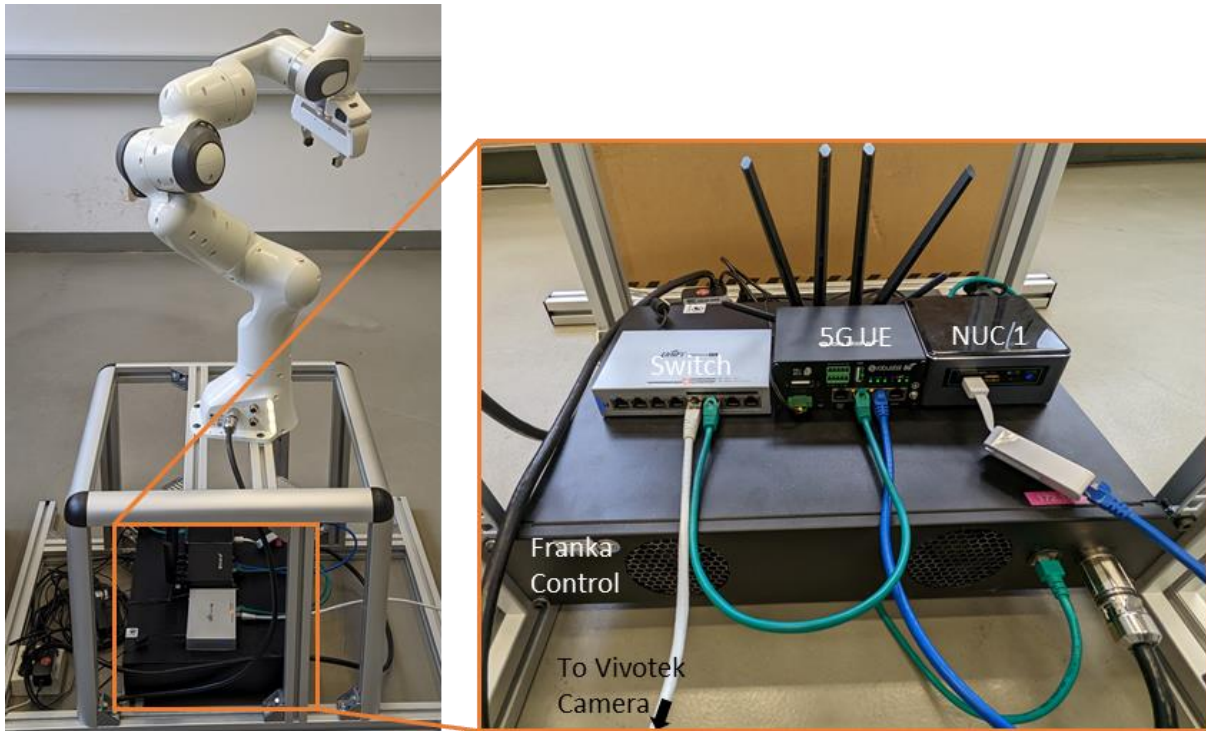


Figure 3-3: Robot unit with 5G UE and NUC1 running the MS.

An overview of all robot control components with the split into MA and MS is given in Figure 3-4. As detailed before, the MS only runs the interpolator, while all other functionalities are offloaded to the cloud controller on the MA. The output of the MA and MS is a joint vector, which is the control data for the robot. The Franka robot has in total seven degrees of freedom and seven axes of motion. On the MA, the joint vector

$$\vec{j}(t) = [j_0(t), j_1(t), j_2(t), j_3(t), j_4(t), j_5(t), j_6(t)]$$

at time t represents the pose of each axis j_i for $i = 0, \dots, 6$ in form of a float number denoting its angle. The cycle time of the MA is $T > 1\text{ms}$, hence a new joint vector is generated each $t = nT$, with $n \in \mathbb{N}$. Based on this data, the MS uses a cubic Hermite spline to generate a joint vector $\vec{k}(\tau)$, where $\tau = n \text{ ms}$. Details about this method are given in [2].

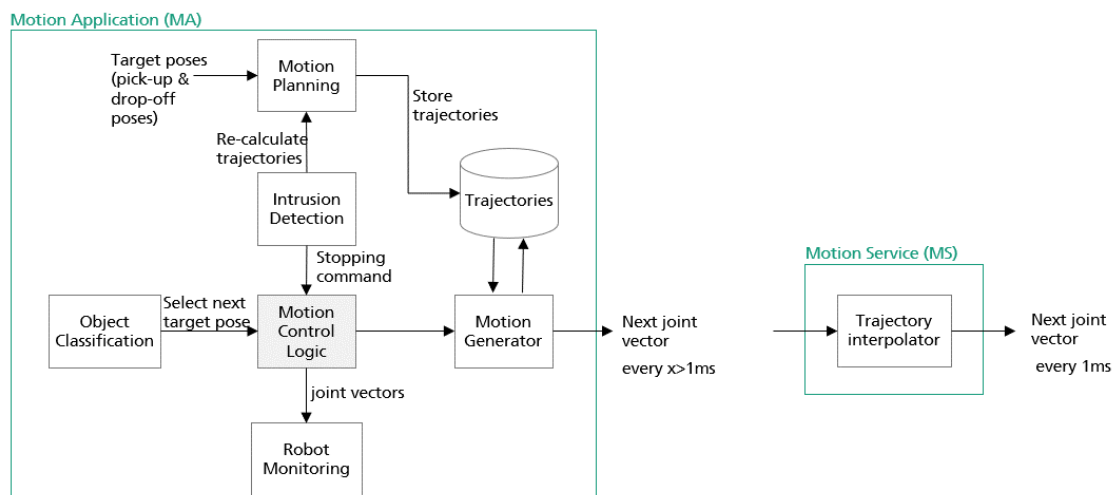


Figure 3-4: Motion Application (MA) and Motion Service (MS) overview.

In the following, we provide a description of each component of the robot UC and how it is integrated into the overall system and software architecture.

3.1.2.1 Motion Planning

The trajectories for the robot are generated with the MoveIt motion planning framework which is based on the robot operating system (ROS) software library. The target poses of the robot are the input for the motion planning, and they are set manually. The robot is brought into the different pick-up locations for the items and to two different drop-off locations. The planning tool receives the target poses and determines a trajectory between the pick-up and drop-off locations using inverse kinematics. The different trajectories are sampled according to a selected cycle time and stored in a database.

It is further possible to add constraints to the motion planning. If there are obstacles in the vicinity of the robot, the trajectories between two target poses can be calculated such that the obstacle is avoided by the robot. This concept is applied for the re-calculation of the trajectory if an intrusion detection event is triggered.

3.1.2.2 Object Classification

The object classification is part of the sorting UC. In manufacturing, robots are often used to pick up parts and take high-resolution photographs in different angles to detect any production faults such as small scratches or deviations in the dimensions of the product. For the purpose of this proof-of-concept setup, we used a simplified classification based on a color code. The items are sorted by the robot according to two different color markings. For the classification, we use the OpenCV library.

3.1.2.3 Intrusion Detection

The intrusion detection is based on the BOSCH cameras video analytics software. The detection software is executed directly on the camera and can trigger alarms accordingly. It supports Open Network Video Interface Forum (ONVIF), which is an open industry standard to achieve interoperability between IP cameras. The camera publishes its alarms using ONVIF to which the robot controller can subscribe. When an intrusion in a predefined area close to the robot is detected, the ONVIF alarm signal is used to stop the robot motion. Furthermore, a re-calculation of the trajectory can be triggered in the motion planning which avoids any detected humans or objects in the vicinity of the robot.

3.1.2.4 Robot Monitoring

A key aspect of this proof-of-concept is the evaluation of the robot motion over 5G. A useful performance indicator is the deviation of the executed trajectory of the robot in comparison to the planned trajectory. To evaluate this parameter, we publish the executed trajectory of the robot using a (Message Queue Telemetry Transport) MQTT broker on the MS at the robot side. The trajectory is given as a time series of joint vectors $\vec{j}(t)$ representing the pose of each joint of the robot. This data is saved in an influxDB on the MA side. Additionally, we store the commanded joint vectors from the MA in the same database and visualize both trajectories and the deviation between them in Grafana. Furthermore, network statistics such as throughput of the network are visualized.

3.1.2.5 Motion Control Logic and Motion Generator

The core of the application is the motion control logic which combines all components of the MA. It is written in python and is responsible to trigger the motion generator to send the correct joint values to the MS. Trajectories are calculated, sampled, and stored in a database, from which the motion generator continuously picks values according to the predefined cycle time T . The motion control logic determines which trajectories the motion generator selects

based on the detected object and if a stopping command is requested by the intrusion detection.

3.1.3 Task List

In line with their definition in Section 4.1.1 of [1] and Section 4.1.4 of [2], we recall here the summarized list of integration tasks that we carried at the UE side.

3.1.3.1 Phase 1

Phase 1 covered the entire year 2021, focusing on interoperability assurance between the NG-RAN infrastructure and the 5GC as well the deployment of the all-in-one solution at the EU factory premises (BOSCH). The time plan in order of task execution for Phase 1 was as follows:

Table 3-2: Task list for Phase 1.

Task	Task owner (in bold) and responsible partners	Labs	Notes
Initial bootstrap of O-RAN Airspan gNB (further on deployed at BOSCH)	HHI	HHI	Preliminary testing of the apparatus (requires integration with a 5GC to work properly).
Pre-configuration and shipment of ATH's 5GC-in-a-box to HHI	ATH	ATH	5GC-in-a-box is the in-factory HW and SW 5GC equipment first pre-integrated with RAN at HHI, then deployed at BOSCH.
In-lab integration of O-RAN Airspan gNB with ATH's 5GC	HHI, ATH	HHI	Integration with 5GC-in-a-box solution succeeded.
In-lab integration of Nokia gNB with ATH's 5GC	HHI, ATH	HHI	Integration with 5GC-in-a-box solution succeeded. Nokia gNB was used at HHI before the availability of ANI's gNB (cf. Section 3.1.1 and 3.2.1)
VPN across sites and on-premises integration plan	BOSCH, HHI, ATH	BOSCH, HHI, ATH	Overall IP plan/service granting/traffic separation discussed among BOSCH/HHI/ATH
Integration of O-RAN Airspan gNB and 5GC-in-a-box at BOSCH Renningen	HHI	BOSCH	First deployment at BOSCH Renningen.

3.1.3.2 Phase 2

In parallel with the completion of Phase 1 activities, Phase 2 started in January 2022, and it included the setup of the on-cloud 5GC instance and the deployment of the 5G edge node (UPF) and ANI's gNB at HHI. The time plan for Phase 2 in order of task execution was as follows:

Table 3-3: Task list for Phase 2.

Task	Task owner (in bold) and responsible partners	Labs	Notes
Integration of 5GS with robot application at BOSCH Renningen	BOSCH	BOSCH	/
Setup of AWS Central Public Cloud solution powered by ATH's 5GC	ATH	ATH	On-cloud 5GC control plane used for cross-site 5G management
Remote integration of ANI's n78 gNB with ATH's 5GC	ANI, ATH	ANI	Remote pre-test integration of ANI's n78 gNB with ATH's 5G core.
Configuration and shipment of ATH's edge node to HHI	ATH	ATH	/
Shipping of ANI's gNB to HHI	ANI	N/A	/
Integration of ANI gNB and ATH edge node in HHI's datacenter	HHI, ATH, ITRI, ANI	HHI	The control plane of the 5GC was hosted on the Central Public Cloud as per the envisioned architecture – cf. Section 3.1.1.
Moving from BOSCH Renningen to the final BOSCH plant	BOSCH, HHI, ATH	BOSCH	Final deployment was successfully carried out in the BOSCH factory.

3.2 Taiwanese System Integration

This section describes the final updates on the progress of system integration in the live industrial environment and the pre-integration activities of ANI's gNB consequently delivered to HHI for the hybrid 5G deployment (cf. Section 3.1.1).

3.2.1 Network Integration

As described in previous deliverable [2], the end-to-end 5G network was deployed into IMTC plant and basic control-plane and user-plane functions are running live properly. To make sure the latency requirements of cloud-based controller can be met, the test item 2.5 reported in [2] was revisited and tested again. The round-trip-time value of ping packets between UE and the application server was improved significantly with min/avg/max/mdev = 10.5/20.5/28.7/5.1 ms. The integration of vertical UCs with 5G system will be reported in Section 4.

In addition, as reported in Section 3.1.1, an additional gNB supplied by ANI was integrated at HHI. To this end, for in-lab testing activities before the installation of the radio equipment at HHI, a remote integration program of ANI's n78 gNB with the on-cloud instance of ATH's 5GC was carried out. The remote test infrastructure is illustrated in Figure 3-5 and consisted in a PPTP-VPN based transport network, connecting ANI's lab to the central public cloud where ATH's 5GC was hosted.

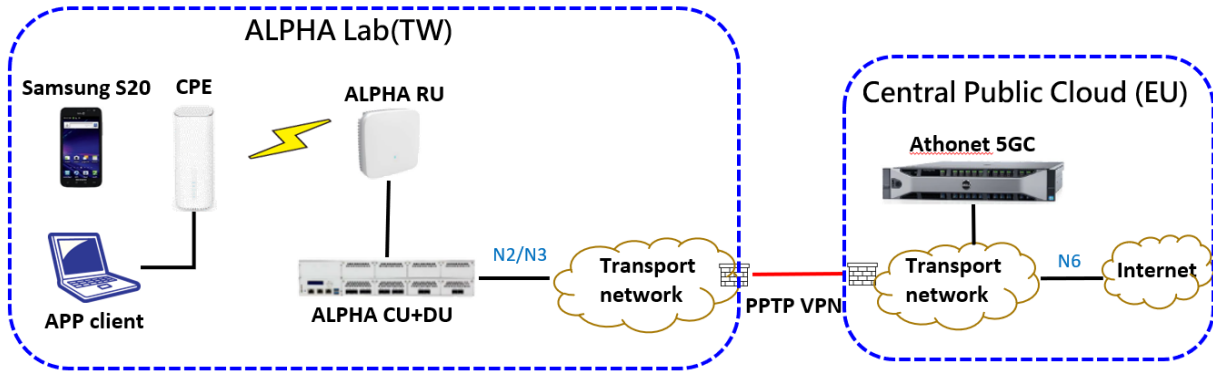


Figure 3-5: Network architecture of remote testing.

The test items reported in Table 3-4 were verified, showing a good level of interoperability between ANI’s gNB and ATH’s 5GC. This test group includes 8 test cases and covers essential procedures when the gNB establishes signaling connection to the 5GC, followed by UE registration and data transfer. In addition, transitions between RRC_CONNECTED and RRC_IDLE states were tested. It should be noted that although the last item was not successfully passed in this in-lab initial interoperability tests, it does not impact the proper operation of the UC if the UE stays in RRC_CONNECTED state. Further, this issue was overcome during the final on-site deployment of the gNB at HHI, and the test item was eventually successful, as reported in Table 3-1.

Table 3-4: Interoperability test items.

TEST ID	TITLE	Test Purpose	Result
1.1	NG Setup	Successful NG interface setup between gNB and 5GC	Pass
1.2	UE Initial Registration with IMSI identity	UE initial registration with IMSI identity	Pass
1.3	UE Initial Registration with GUTI identity	UE initial registration with GUTI identity	Pass
1.4	PDU Session Establishment	Successful establishment of the PDU session	Pass
1.5	Data Transfer using Ping application	Successful data transfer between the UE and external data network (e.g. 8.8.8.8)	Pass
1.6	UE Deregistration	Successful deregistration procedure triggered by the UE entering flight mode	Pass
1.7	Access Network Release	AN release due to user inactivity	Pass
1.8	UE-Triggered Service Request	Successful MO (Mobile Originated) Service Request	Fail

3.2.2 Task List

Analogously to Section 3.1.3, we report here for completeness and as a reference to the reader the list of integration tasks that have led to the full integration of the TW setup. The tasks and the phases mentioned therein were defined in Section 4.2.3. of [1] and Section 4.2.3 of [2].

Table 3-5: Task list for in-lab and on-premises integration.

Task	Task owner (in bold) and responsible partners	Labs	Notes
Phase 1 test cases with configuration A verified after 5GC upgrade	ITRI , ANI, III	ITRI	Phase 1 and 2 with configuration A and C were verified to ensure the E2E system was working properly, which covers RAN, 5GC, and MEC.
Phase 2 test cases with configuration A verified	ITRI , ANI, III	ITRI	
Phase 1 and 2 test cases with configuration C verified	ITRI , ANI, III, CHT	ITRI	
On-premises integration plan	ITRI	N/A	The physical system architecture of the shop floor was identified, which included 5G system, transport network, and OT/CT integration.
On-premises 5G system integration	ITRI , ANI, III, CHT	ITRI	The 5G network was deployed into IMTC plant and basic control-plane and user-plane functions are running live properly.
Phase 3 test cases verified on the premises	ITRI , ANI	ITRI	The traffic profile of UCs was incorporated to make sure the throughput and latency requirements will be met.
Software of additional UC (cloud controller) virtualized and integrated to MEC platform	ITRI , CHT	CHT, ITRI	The industrial KPIs were monitored by CHT's ECore-Cloud platform via SNMP protocol.
Integration of 5G with additional CBC UC	ITRI , ANI, III, CHT	ITRI	/
Integration of 5G with combined UC-1 and UC-2	ITRI , ANI, III, CHT	ITRI	/

3.3 End-to-end System Integration

3.3.1 Final Architecture

In [1] and [2], we have extensively described the architectural components that constitute the interconnected EU and TW 5G networks. For the reader's convenience, we simply recall the main features of such architectures in Figure 3-6 and Figure 3-7, and we refer the reader to previous deliverables for further details. Notice that the dashed lines that interconnect the 5GC's Authentication Server Functions (AUSF) and UDM instances, represent the unification

of the subscriber profile management modules via the common centralized provisioning system introduced in Section 2.2 of [2] and further described in Section 3.3.2.

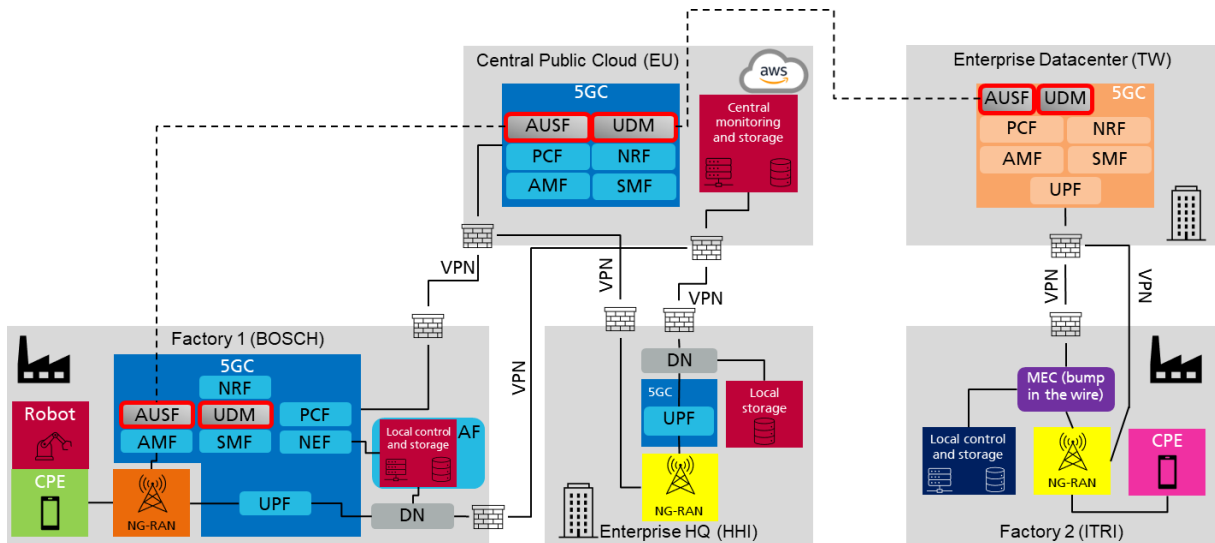


Figure 3-6: EU-TW joint setup.

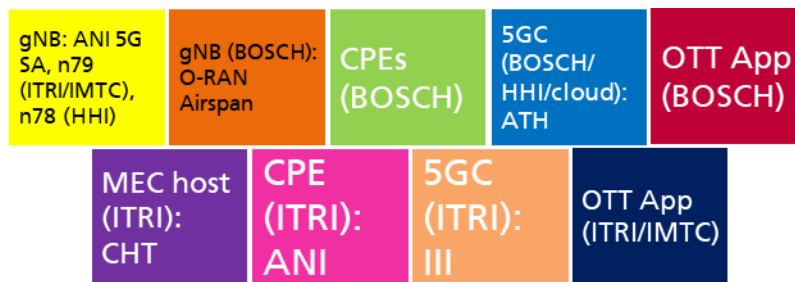


Figure 3-7: Legend of the architectural components of the EU-TW joint setup (in parentheses, the physical locations of each item).

3.3.2 5GC Unified Provisioning System Implementation

In Section 2.2 of [2], we explained how the EU and TW 5G networks are interconnected leveraging a synchronized UE provisioning and management system, developed by the project's partners. Such a centralized Operations, Administration, and Maintenance (OAM) system is designed and implemented for managing physically separated 5G Systems (5GSs), as shown in Figure 3-8. Currently the OAM is located in Taiwan and accesses ATH's EMS, located in Europe, via an OAM adaptor and ATH's function node access module (see Figure 3-9).

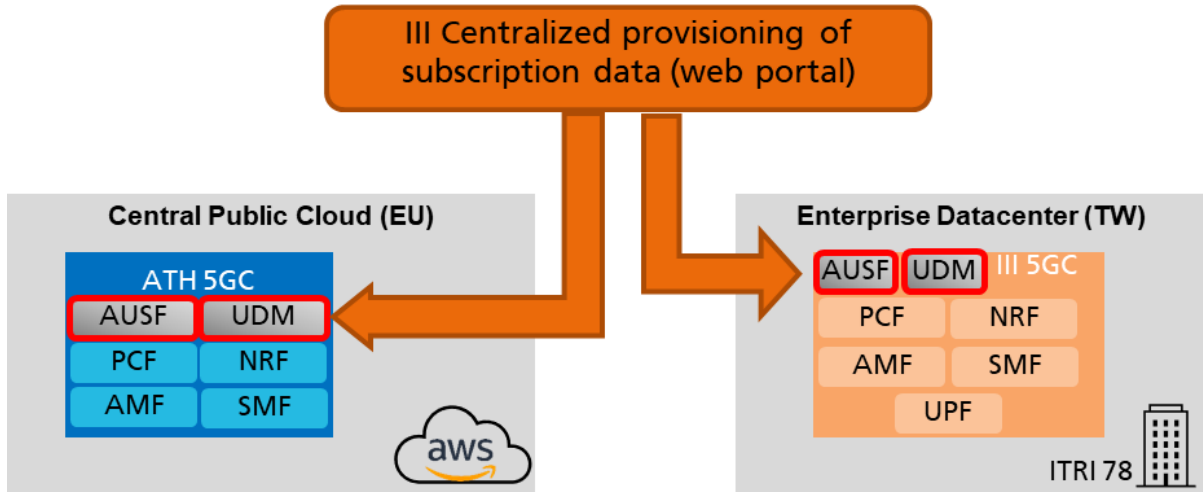


Figure 3-8: Centralized OAM for distributed 5GS management.

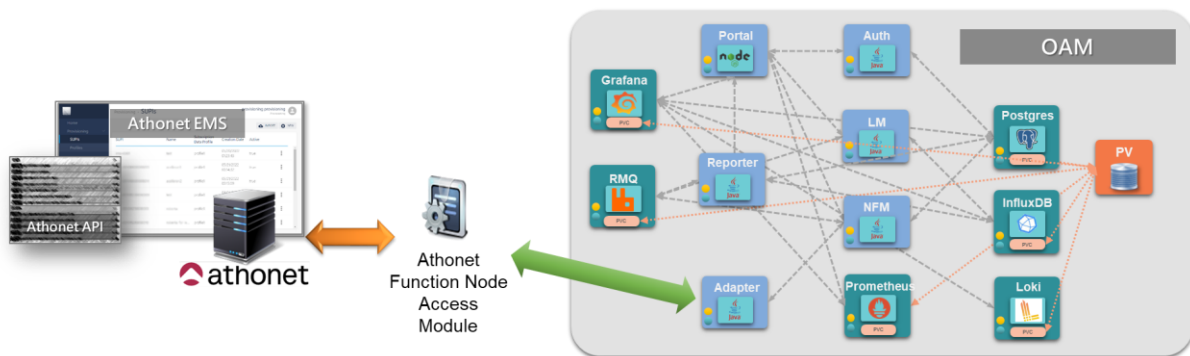


Figure 3-9: Remote access mechanism.

We complement in this document the information provided in [2], that focused on the UE provisioning and OAM system of the TW part of the intercontinental unified network architecture. Via the features developed in the last part of the project, the unified provisioning system was extended to manage also the users of the EU side. This happens leveraging the APIs of ATH's 5GC.

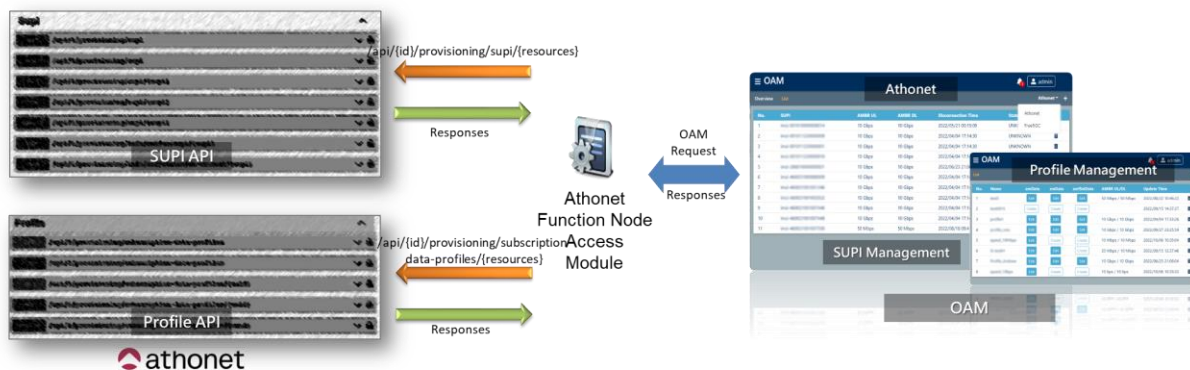


Figure 3-10: RESTful APIs for remote configuration and management.

In particular, ATH’s 5GC can be configured and managed by RESTful “SUPI” and “Profile” APIs. SUPI stands for Subscription Permanent Identifier, as defined in [8]. SUPI is a 5G globally unique ID allocated to each subscriber. Both III and ATH’s 5GC can be configured and managed by RESTful APIs SUPI and Profile (see Figure 3-10).

SUPI APIs are designed for:

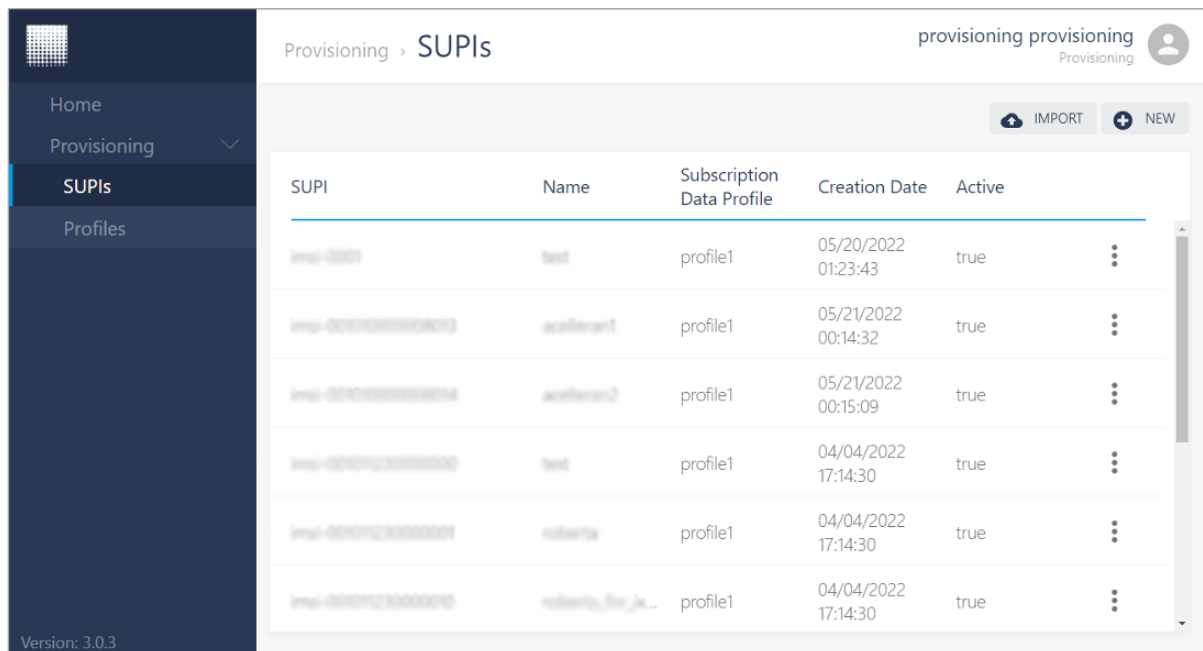
- UE creation, delete, and modification.
- UE authentication settings: IMSI (International Mobile Subscriber Identity), K, OP.
- Association of UEs with existing profiles.

Profile APIs are designed to manage:

- QoS settings: AMBR (Aggregate Maximum Bit Rate), NSSI (Network Slice Subnet Instance), 5QI (5G QoS Index), ARP (Allocation and Retention Priority).
- Access management, session management, and SMF selection.

The 5GC network instances and the unified provisioning system involved in the intercontinental setup are physically separated but connected via VPN. The web-based centralized OAM was implemented and tested first with ATH’s on-cloud 5GC. All APIs, both SUPI API set and Profile API set were successfully tested.

While operating the system, an administrator has to create profile(s) before SUPI creation. A SUPI (i.e. UE) is associated (by selection) with an existing profile, which contains the information of access (Figure 3-12), session (Figure 3-13), and SMF (Figure 3-14). The QoS parameters, such as allowed up-link/downlink peak data rate, priority, resource preemptable or non-preemptable, etc., can be well defined in the session management UI (Figure 3-13).



SUPI	Name	Subscription Data Profile	Creation Date	Active
imsi-0001	test	profile1	05/20/2022 01:23:43	true
imsi-00100000000001	subscriber1	profile1	05/21/2022 00:14:32	true
imsi-00100000000004	subscriber2	profile1	05/21/2022 00:15:09	true
imsi-00100000000000	test	profile1	04/04/2022 17:14:30	true
imsi-00100000000000	subscriber	profile1	04/04/2022 17:14:30	true
imsi-00100000000000	subscriber_for_je...	profile1	04/04/2022 17:14:30	true

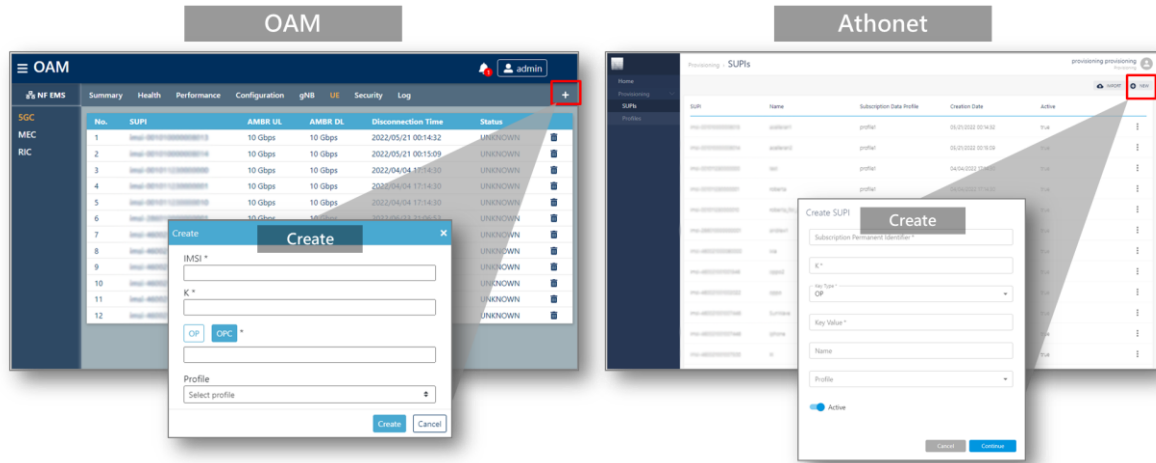


Figure 3-11: OAM UI.

Figure 3-11 shows a snapshot of a SUPI creation. The required inputs are IMSI, K, OP (or OPC), and an associated profile by selection. Each profile has its own Access Management Data (Figure 3-12), Session Management Data (Figure 3-13), and SMF Selection Data (Figure 3-14).

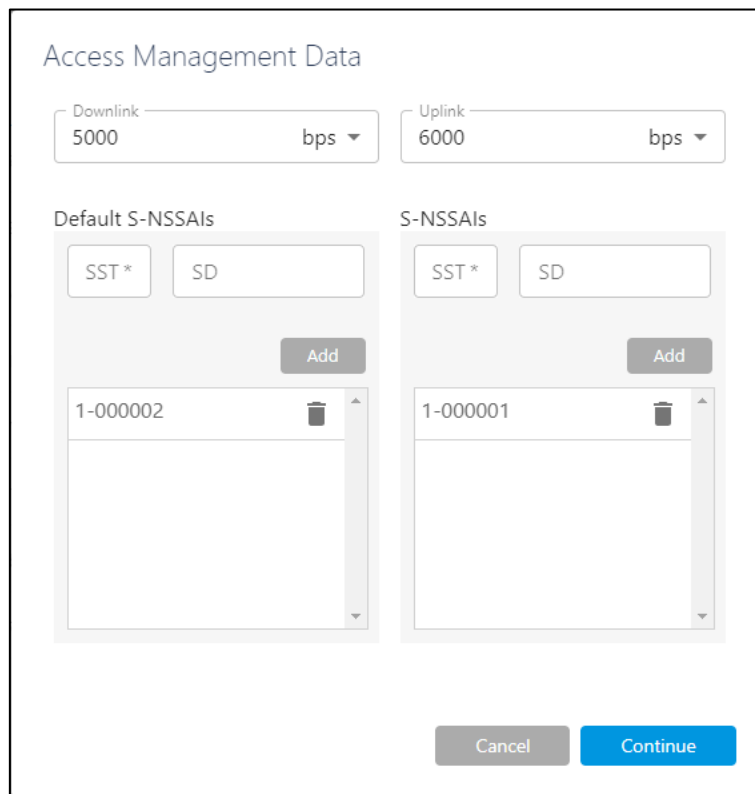


Figure 3-12: Access management UI.

Session Management Data

Add S-NSSAI

1-000002 🗑️ ^

SST: 1 SD: 000002

Add DNN Configuration

DNN-test 🗑️ ^

DNN name: DNN-test

Downlink: 10 bps Uplink: 10 bps

5G QoS Identifier: 1 Preemption Capability: NOT_PREEMPT

Preemption Vulnerability: NOT_PREEMPTABLE ARP priority level: 1

QoS priority level: 1

ATSSS Allowed

Figure 3-13: Session management UI.

SMF Selection Data

Subscribed SNSSAI Infos *

SST name *

Add

1-000001 🗑️ ^

DNN name * DNN-test Default DNN

Add

- DNN-test 🗑️

Figure 3-14: SMF selection UI.

3.3.3 Task List

We conclude in this section the summary of the main design, integration, and experimentation tasks carried out throughout the project duration, with those specifically dedicated to the E2E intercontinental integration. As for Section 3.1.3 and Section 3.2.2, the tasks in the following table are reported as defined in [2].

Table 3-6: Task list for end-to-end integration.

Task	Task owner (in bold) and responsible partners	Labs	Notes
Final decision on E2E application design	ITRI, BOSCH	N/A	Alignment needed between the owners of the workshops (IMTC and BOSCH factory).
Integration of centralized common UE provisioning system with III and ATH's 5GCs	III, ATH, ITRI	III, ATH	The web portal developed by III is able to provision subscription data into III and ATH's UDMs via RESTful APIs.
E2E application up and running at both workshops	ITRI, BOSCH	ITRI, BOSCH	/
Start of inter-site UC integration with local 5GS	ITRI, BOSCH	ITRI, BOSCH	Integration of application and 5GS at trial site.
E2E testbed validation	ITRI, ANI, III, CHT, BOSCH, ATH, HHI	ITRI, BOSCH	Validation of the EU-TW E2E 5G testbed with the inter-site UC.
Experimental results collection	ITRI, ANI, III, CHT, BOSCH, ATH, HHI	ITRI, BOSCH	Reported in D5.3.
Finalization of trials and inclusion of results in D5.3	ALL	N/A	/

3.4 Timeline of the Task Lists

Finally, this subsection contains a graphical summary of the timeline of the task lists devoted to the EU, TW, and intercontinental testbeds in the period covered by this deliverable. Each task in the graph is marked as '[EU]', '[TW]' or '[EU/TW]' according to the testbed it refers to.

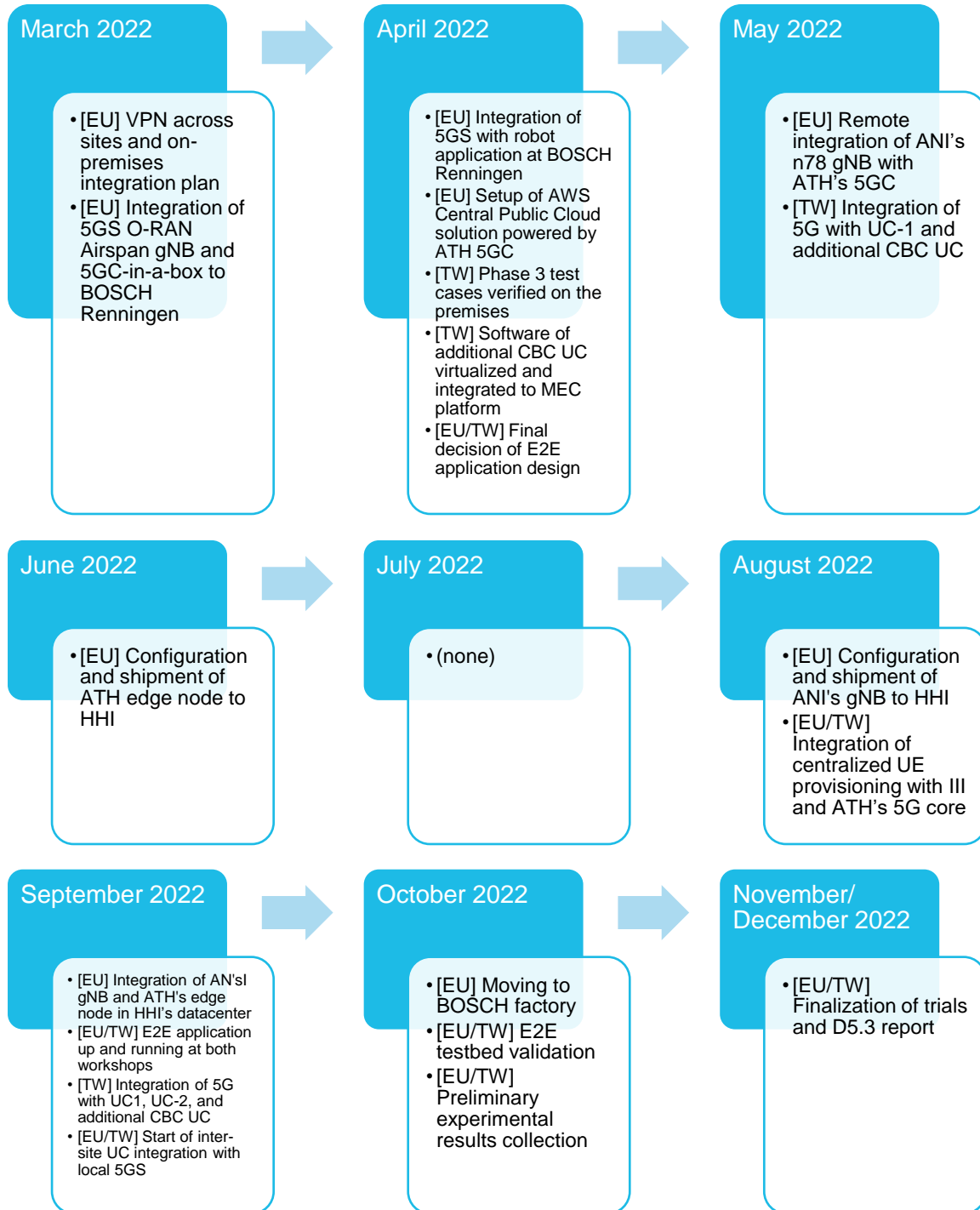


Figure 3-15: Graphical representation of WP5's implementation, integration, testing, and validation activities in the period covered by this deliverable.

4 Final Performance Measurements and Analysis

In the following of this section, we provide, on a per-UC basis, a report of the performance measurement campaigns and some analysis of such results in order to draw the conclusions of the piloting activities carried out in the 5G CONNI project.

4.1 European Testbed

4.1.1 Network

In Section 4.1.1 of [2], we presented results on the achievable throughput in downlink (DL) and uplink (UL) using *iPerf*. Due to a wrong configuration resulting in the usage of lower MCS during data transmission, we only measured 150 Mbps throughput in downlink using TCP. In the current setup, this configuration was fixed, resulting in an increased DL throughput of up to around 280 Mbps, as shown in Figure 4-1. The UL throughput is unchanged to the previous report and peaks at around 45 Mbps.

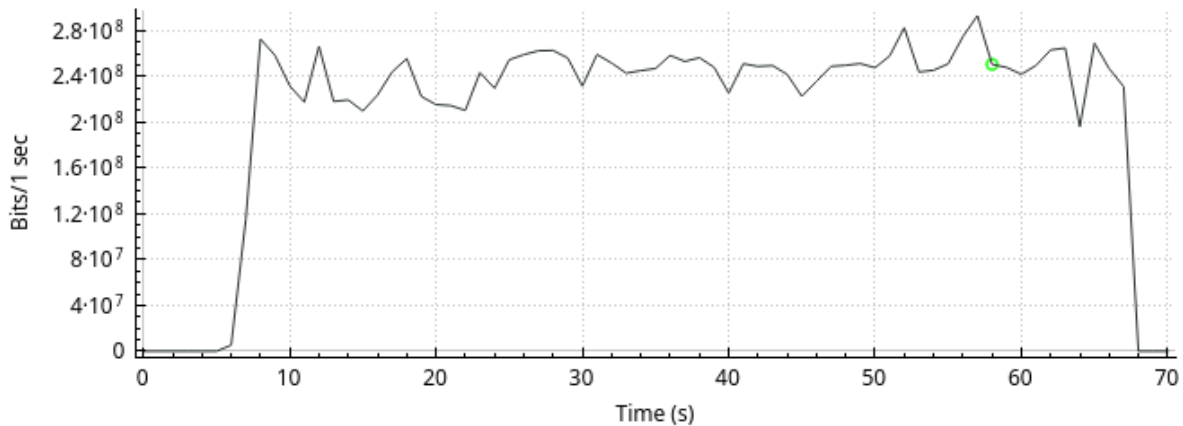


Figure 4-1: Downlink network throughput.

In the EU testbed, we measured a peak throughput of 280Mbps in downlink as shown in Figure 4-1.

4.1.2 UC-3: Robot Platform with Edge Intelligence and Control

The evaluation of UC-3 consists of two main parts, first we verify the functionality of all system components and describe in detail the workflow of the robot. Second, we analyze performance metrics on the network and application level by tracing the communication, as well as evaluating the robot motion trajectories, respectively.

4.1.2.1 Workflow of Robot

The task of the robot is to pick up items from the pick-up area and sort them into two different boxes as shown in Figure 4-2. To perform this task, the MA connected to the N6 interface of the 5G system runs multiple system components as described in Section 3.1.2.

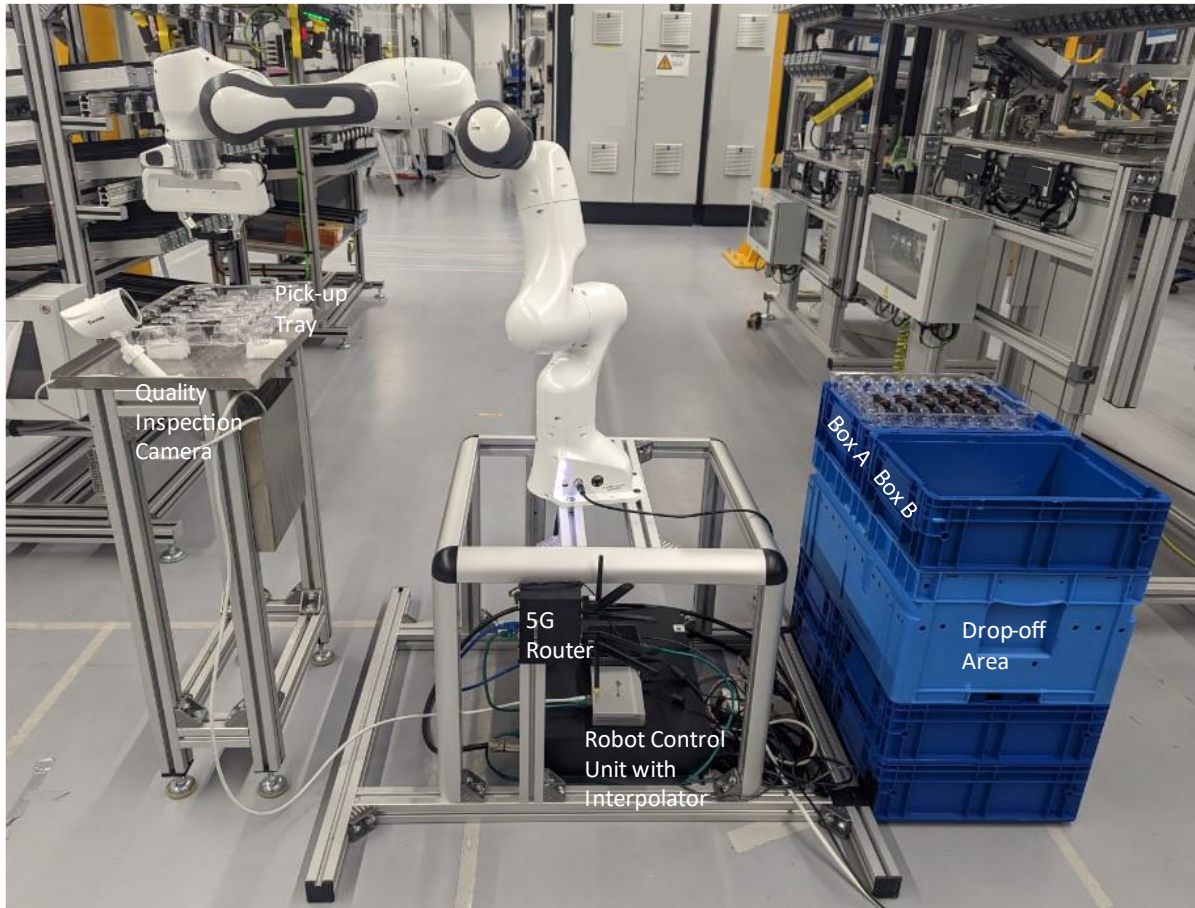


Figure 4-2: Robot setup for sorting application.

The principal workflow of the MA controller with the different process steps for the sorting application is shown in Figure 4-4 on the left-hand side. The key component of the MA is the motion control subroutine on the right-hand side marked in blue. It is the only time-critical part of the application and responsible to determine the next joint vector $\vec{j}(t)$ within the given cycle time. Each step in the workflow on the left side requiring the robot to move to a target destination initiates this motion subroutine.

The workflow of the robot is initiated by determining the different target locations, i.e., the drop-off and the pick-up locations. The user moves the robot manually to the different target poses and the MS reports these poses back to the MA. Based on this information, the motion planning tool determines the trajectories between target poses.

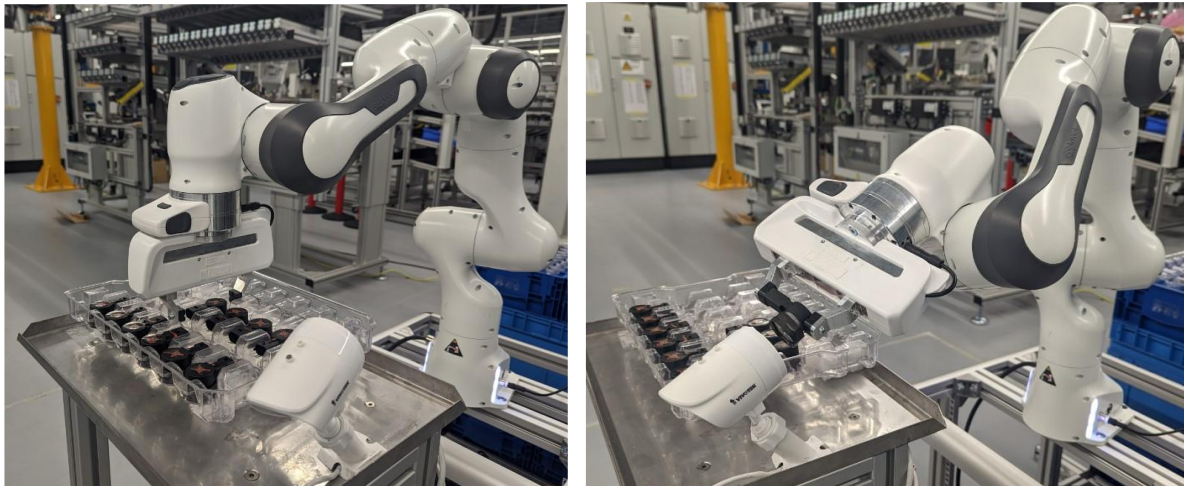


Figure 4-3: Robot picking item up (left) and moving it in front of the camera (right).

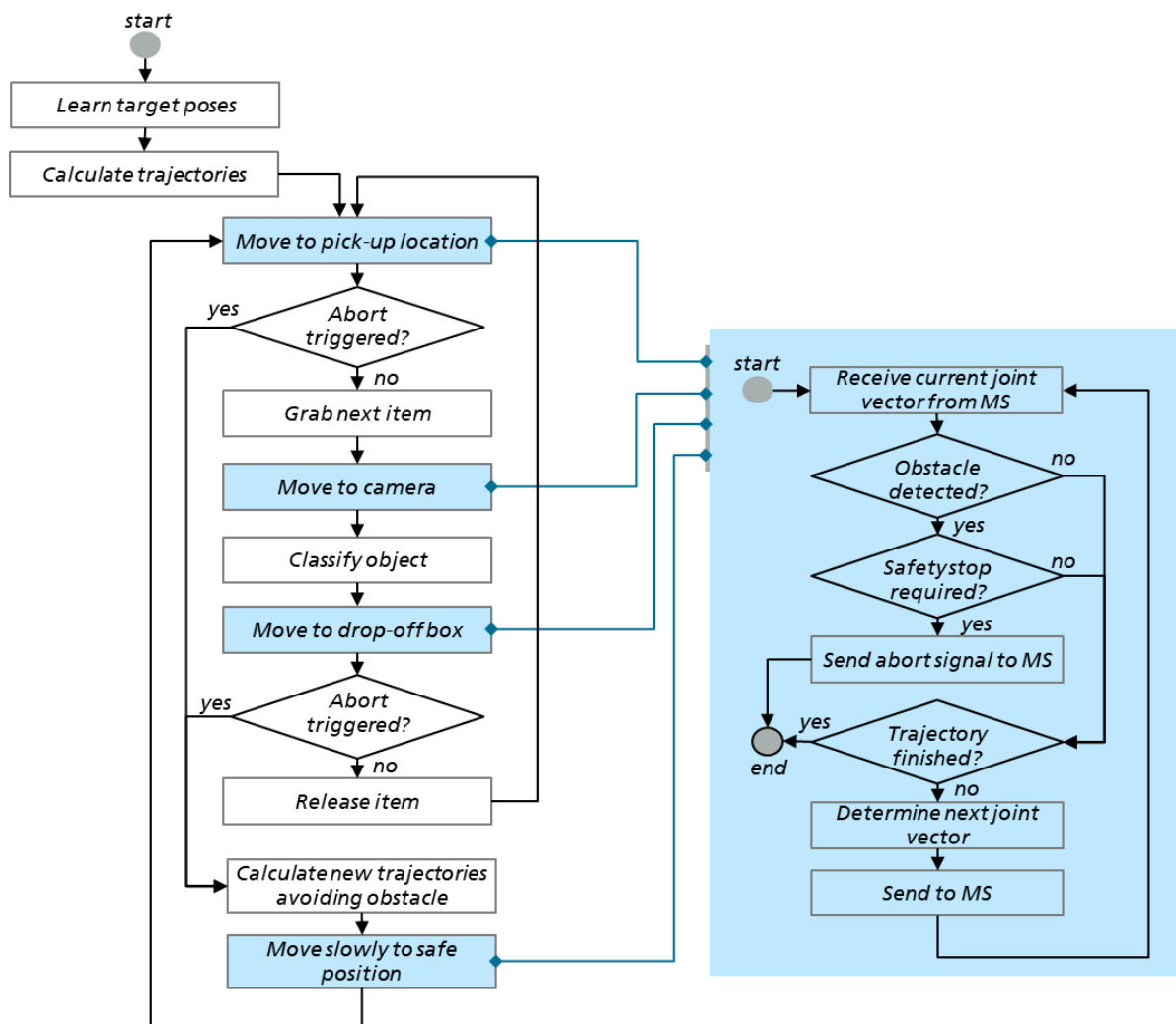


Figure 4-4: Workflow of robot.

A screenshot of the initial motion planning is given in Figure 4-5. It shows the two different drop-off locations, the camera position for the object classification and the pick-up locations. The dimensions of the pick-up tray are known, hence only the pose to grasp the first item is

required to compute all trajectories. After the initialization, the robot will collect the first item and moves it into the field of vision of the camera (cf. Figure 4-3).

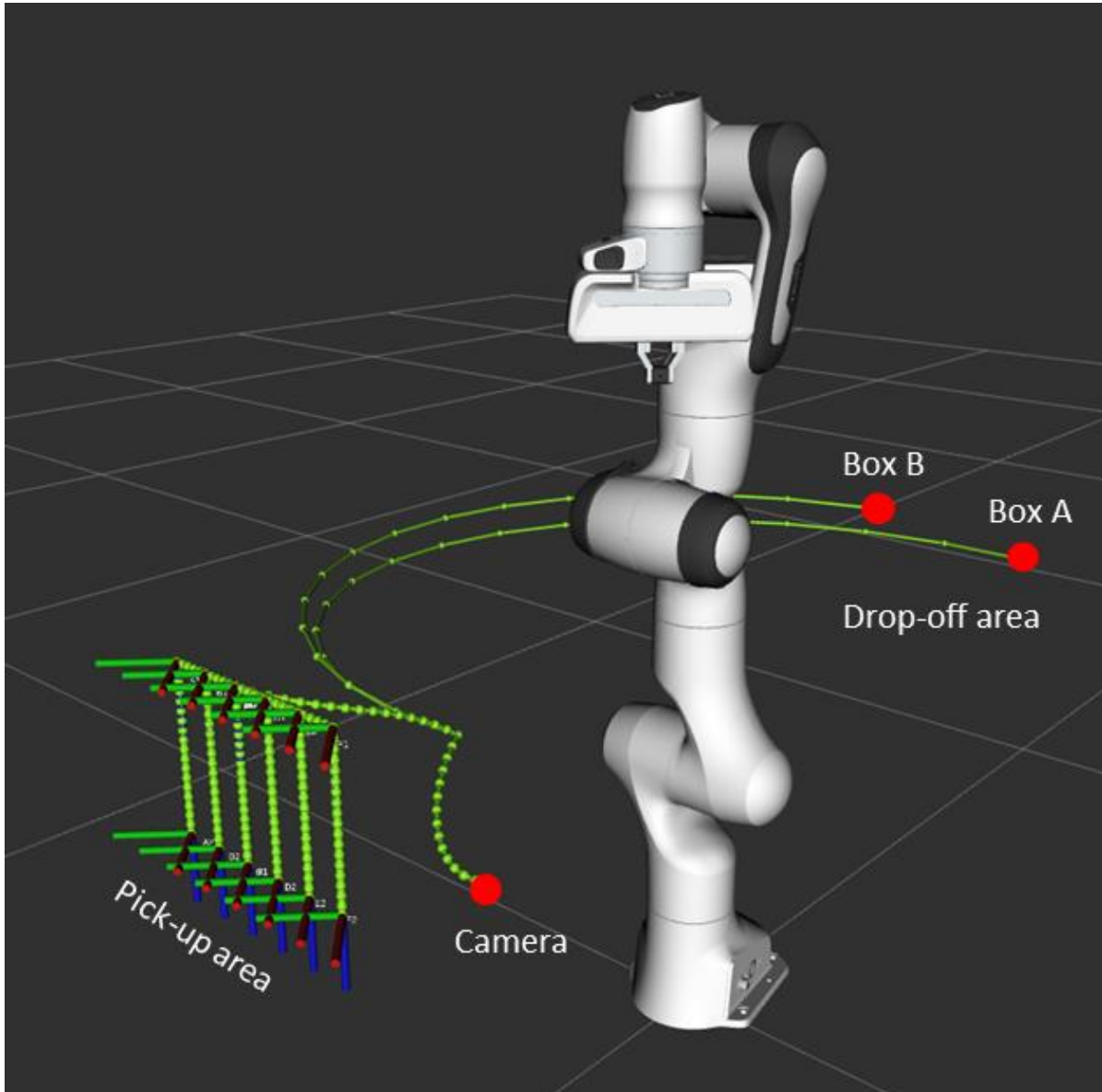


Figure 4-5: Output of motion planning tool.

The items sorted by the robot are parts of an automotive injection nozzle. Usually, these items have high requirements on precise manufacturing to guarantee tightness of the valve. Visual quality control is commonly used in this area, which we are demonstrating with this application. We simplified the object classification by equipping each item with a color marking on the back. The MA recognizes the indicator and determines the corresponding trajectory to move the item to the correct box. To save bandwidth on the 5G link, the MA only pulls this video stream from the camera in this process step. The measured bandwidth requirement of the camera is around 2 Mbit/s.

After the item is dropped off, the robot moves back to the pick-up area to select the next item.

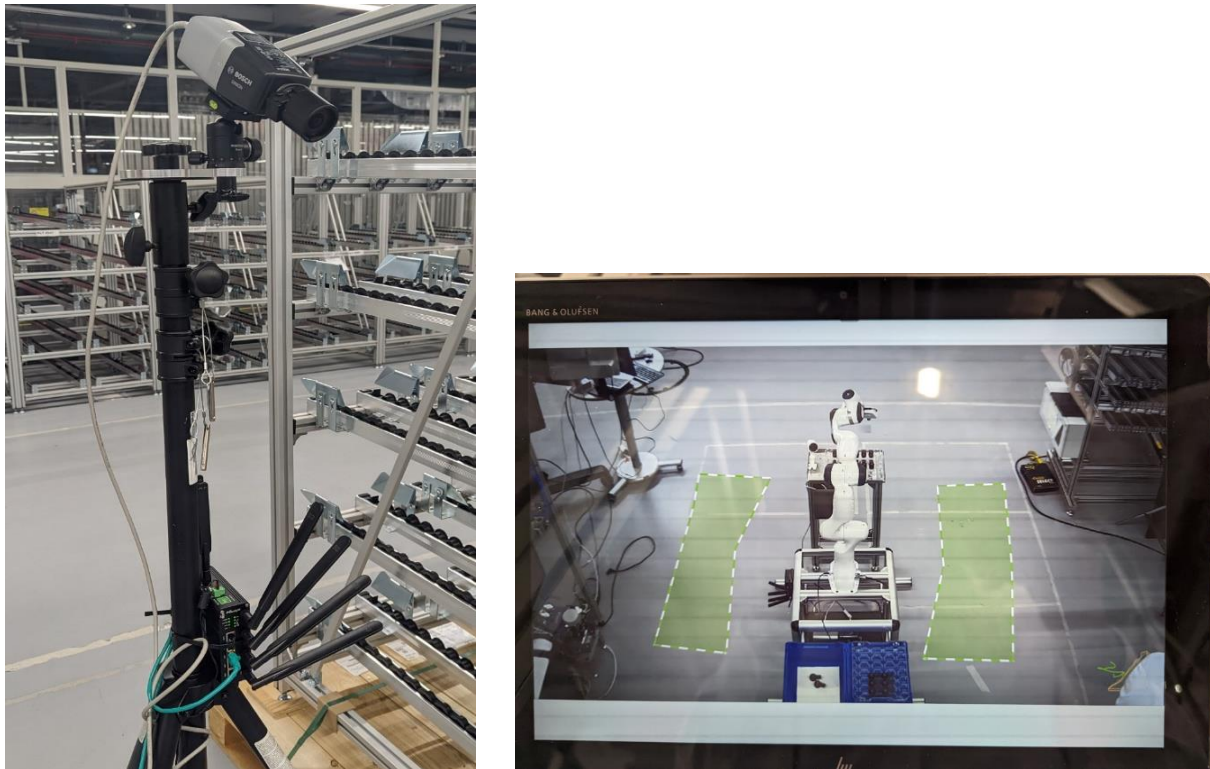


Figure 4-6: BOSCH Dinion Camera with video analytic connected over 5G router (left) and detection areas for intrusion alerts around the robot (right).

For each of the motion tasks, the motion control routine is called to determine the next joint vector and send it in a timely manner to the MS. Furthermore, in the motion control routine, the intrusion alarms from the BOSCH camera are checked each cycle to detect objects in the area around the robot (Figure 4-6). If the current motion of the robot would potentially be obstructed by an object, the MA should stop the motion immediately and find a new route to the target pose. The integration into the MA happens via the ONVIF protocol which provides a simple interface to video analytics software of the camera. Since the video is processed directly on the camera, we do not even necessarily require streaming the video to the MA. Sending only the meta data requires only very low bandwidth in the range of several kbit/s. The usage of cameras with on-device computation is hence a very suitable in a wireless scenario. The camera is connected via an individual 5G module and has hence the advantage that it can be set up flexibly in the factory to provide an unobstructed field of view on the robot (Figure 4-6). For our demonstration purpose, we defined two areas of interest for the video analytics. If a person is detected in one of those areas, the motion is halted, and the motion planning tool determines a new set of trajectories. First, the robot arm is slowly retracted away from the person or object into a safe position. Second, an alternative trajectory to the drop-off locations by avoiding the triggered area aside the robot is calculated (Figure 4-6).

This type of application benefits greatly from the offloaded control architecture as the MA acts as a central instance that receives all the relevant data from the individual devices, i.e. the camera and the robot. This is especially the case if extending this UC to multiple robots and cameras in overlapping areas.

The last important function block in the robot application is the monitoring GUI implemented in Grafana. It shows relevant parameters in real-time to assess the performance and status of the robot. The GUI visualizes the trajectories, as well as network-related statistics.

On the application level, we can trace the movement of the robot in terms of the seven joint positions. We take 10 data points each second for the commanded trajectory, as well the executed trajectory by the robot. This further allows to determine derivations of it such as the speed and acceleration of each joint. Figure 4-7 shows the GUI and depicts the commanded joint vector, the mean deviation between all commanded joints from the executed joints, and the speed of each joint in radians per second. The deviation shown in the plot is dominated by the time delay in execution of the motion due to the interpolation. Hence the visible correlation between the deviation and the absolute speed of the joints. The time delay can be compensated to determine the exact motion deviation in post-processing, as presented in the subsequent evaluation part. The key takeaway here is that if there is no motion, the commanded and executed trajectory are matching with zero deviation, meaning that the target pose is always reached with high accuracy. This data is continuously saved in the influxDB and serves also as the basis for the analysis in the later evaluation part of this section.

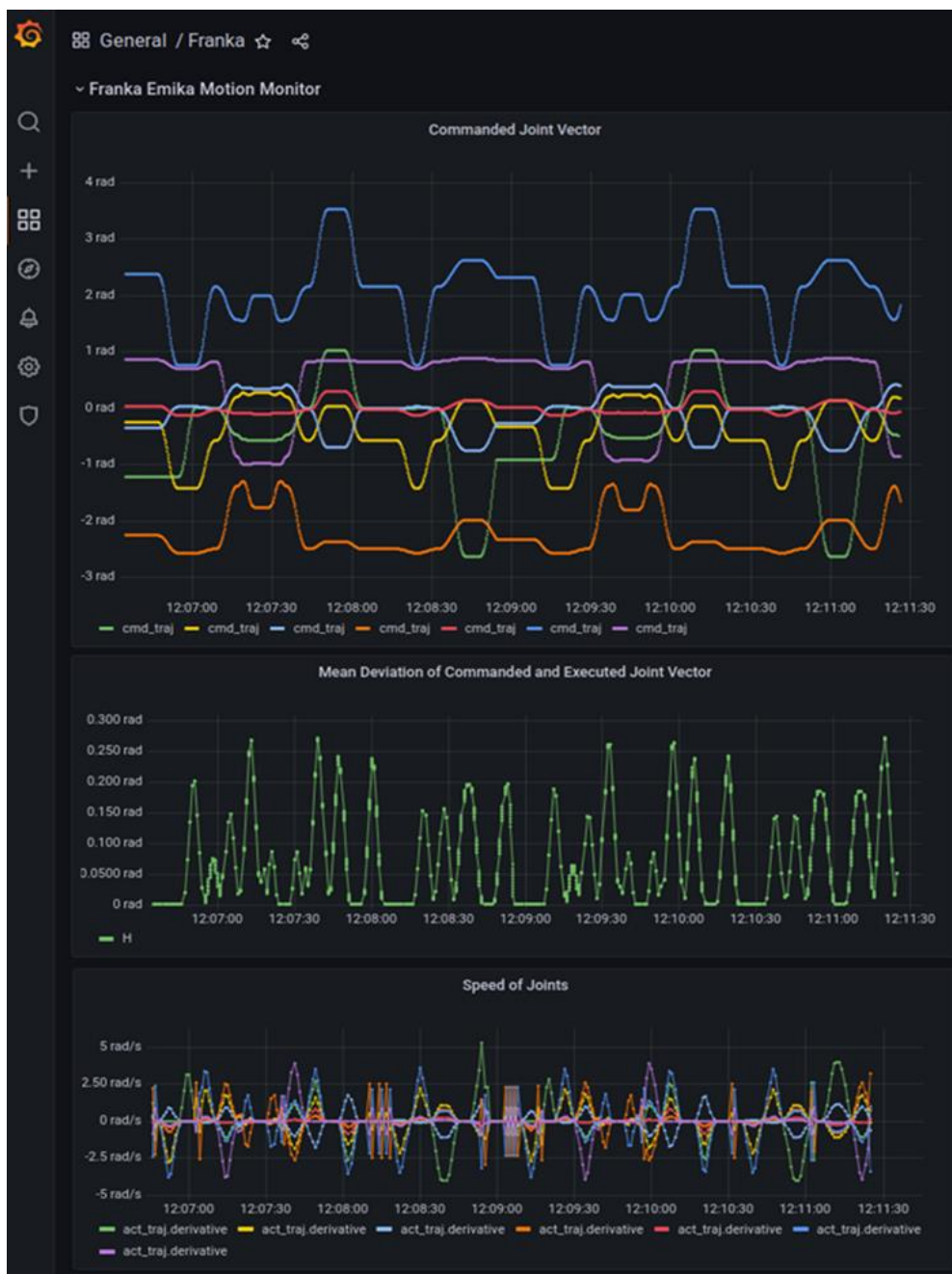


Figure 4-7: Trajectory monitoring in Grafana.

We also display some network properties in Grafana such as the transmitted and received data rate between MA and MS. Note that it only captures the interface statistics of the MA using Telegraph, hence packet losses over 5G in TX are not accounted for. In Figure 4-8, two distinctive peaks with 2 Mbit/s in RX and 60 kbit/s in RX can be observed. These are caused by the Vivotek camera which is activated in the object classification step. If not in use, the camera is turned off. During normal operation, we can see that the control stream from the MA only generates about 15 kbit/s of data. Additionally, an approximate round-trip time is visualized using a background ping command to check the sanity of the network.

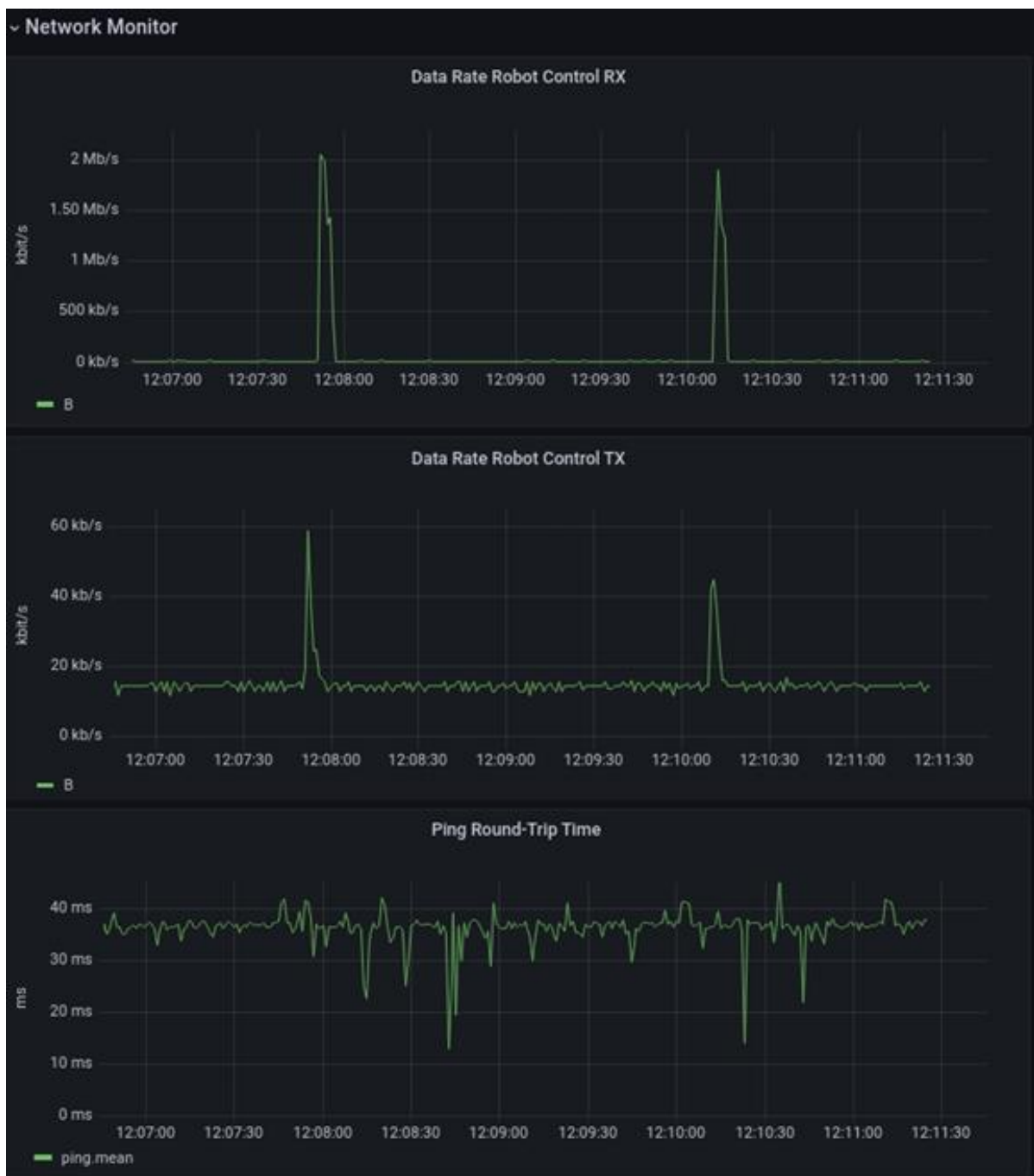


Figure 4-8: Network monitoring in Grafana.

4.1.2.2 Performance Evaluation

The focus of the evaluation is to investigate the impact of the 5G network on the robot performance. Especially, if there is any measurable degradation in the execution of the motion tasks when operating the robot wirelessly.

4.1.2.2.1 Evaluation KPIs

To quantify the performance, we capture network and application statistics, which are partly already presented in Grafana as described in the previous section.

The relevant data for the trajectory evaluation are the commanded and executed trajectory values which are captured throughout operation by the MA in a database alongside with a timestamp. From these trajectories, we define the following KPIs for evaluation.

Joint Speed

As described in 3.1.2, the commanded trajectory is given as a joint vector $\bar{j}(t)$. The executed trajectory reported by the MS is denoted $\bar{k}(t)$. The sampling of the vector $t = nT$ depends on the cycle time, throughout the evaluation we use $T = 100\text{ms}$. For each joint j_i and k_i with $i = 1, \dots, 7$ we can determine the speed $v_{j_i}(t)$ of joint i as

$$v_{j_i}(nT) = \frac{j_i((n+1)T) - j_i(nT)}{T}.$$

The speed of the executed trajectory $v_{k_i}(t)$ is determined in the same way.

Joint Speed Deviation

The deviation in joint speed between the executed and commanded trajectory is defined as

$$d_v = |v_{j_i}(nT) - v_{k_i}(nT)|.$$

We furthermore use different representation of it such as the complementary cumulative distribution function $ccdf(d_v)$ and the standard deviation $std(d_v)$.

The network statistics are captured by additional network trace capturing devices. We use ProfiShark 1G+ network taps (cf. Figure 4-9). The taps capture each packet and add a precise hardware timestamp. The clocks of both taps are synchronized via a Pulse Per Second (PPS) signal and provide an accuracy in the double-digit nanosecond range. With this setup, we can determine several network KPIs.

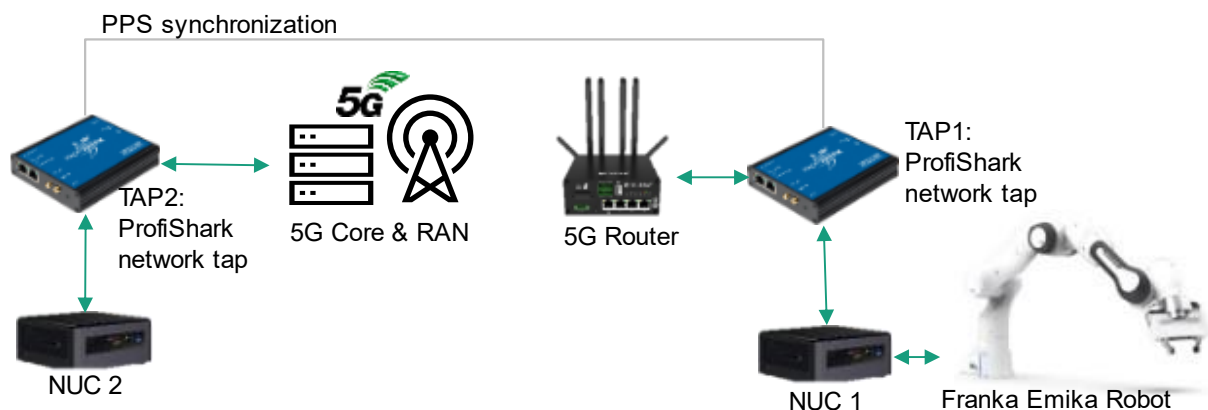


Figure 4-9: Setup for network performance evaluation of UC-3.

Each packet exchanged between NUC1 and NUC2 must eventually pass both TAP1 and TAP2. If a packet is only observed at either one of the taps, the packet must have been lost in the network. Since each packet carries a unique ID i , we can detect any packet losses inside the network.

Transmission Delay

The transmission delay is determined by capturing the timestamp of a frame at TAP1, i.e. T_i^{TAP1} and at TAP2, i.e. T_i^{TAP2} . If the frame is in uplink, the transmission delay is given by $d_{UL} = T_i^{TAP2} - T_i^{TAP1}$. For a downlink frame, we have $d_{DL} = T_i^{TAP1} - T_i^{TAP2}$.

Transfer Interval Time

The transfer interval is the time between two consecutive packets. This is an useful metric to verify that the MA sent out the joint vectors in a timely manner. Furthermore, we can visualize how evenly packets arrive at the MS after being exposed to varying transmission delay on the network.

Measurement results

The main objective of the measurement analysis is to quantify the impact of the wireless network on the robot motion. To investigate different network conditions, we introduce cross-traffic between the MA and MS in downlink additionally to the normal robot control loop. The background traffic is generated by iPerf3 and uses UDP. We gradually increase background traffic from 0 Mbps to 150 Mbps evaluate the different KPIs presented in the previous section.

The control application generates a constant data stream of 10 frames per second, given the selected $T = 100\text{ms}$ cycle time. The data rate is below 15 kbps in downlink, as shown in Figure 4-10. The same rate is observed in uplink, since each motion control frame triggers a feedback frame of the current robot state back to the MA.

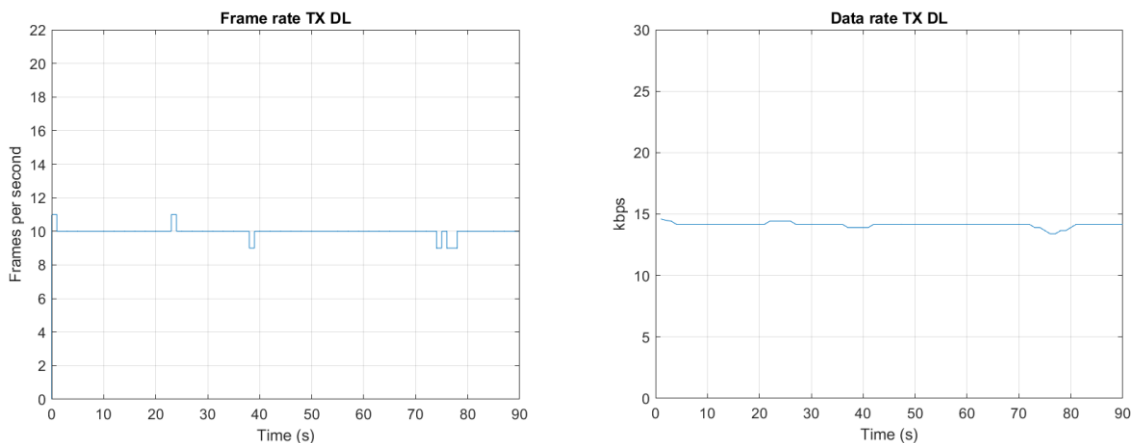


Figure 4-10: Frame rate and data rate of control packets between MA and MS.

We investigate the impact of background traffic on the 5G system for 0, 20, and 150 Mbps background traffic as an example for the ideal condition and the mid and high-utilization scenarios of the 5G network. We look at three key indicators, i.e., the latency, the transfer interval-time at the transmitter side (which is after the egress port of the MA) and the transfer interval time at the receiver side (which is before the ingress port of the MS). These indicators are used to determine how much jitter is added to the control frames and to what extent the 5G system contributed to it.

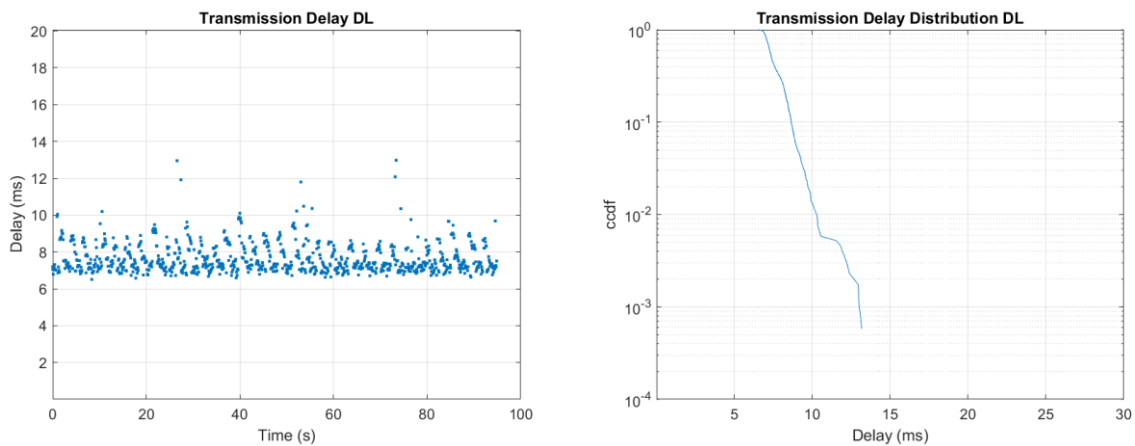


Figure 4-11: DL latency of motion control frames with 0Mbps DL cross-traffic.

In Figure 4-11, the downlink latency over 5G over a duration of 100 seconds is shown. There is no background traffic present, and we can see that there is very limited variation in the latency. The CCDF hence has a steep decline and indicates a less-than-10 ms latency for 99% of the packets.

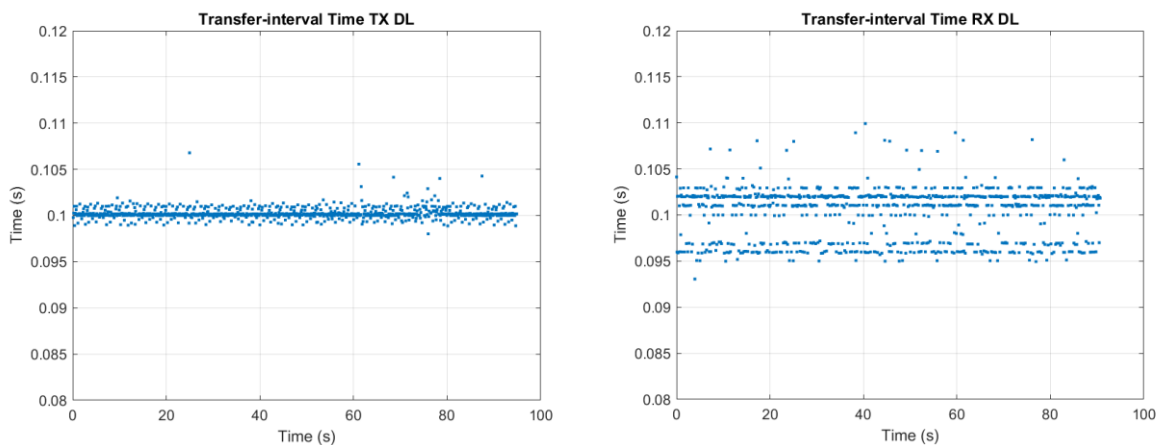


Figure 4-12: Transfer-interval time measured after MA (left) and before MS (right) with 0Mbps DL cross-traffic.

Figure 4-12 shows the transfer-interval time on the MA on the left side. We can observe already here that the MA does not send out data with perfect accuracy according to the 100ms cycle time. This is expected since we use standard hardware without accurate time-synchronization or the use of real-time protocols. Hence, we need to take into account that the jitter observed at the receiver side after transmission over 5G (right picture) is not completely (but for the most part) caused by the 5G system. The transfer interval experienced at the receiver side (right) shows – to some extent – a symmetric behavior around the target transfer interval of 100 ms, which is due to the fact that there is no on-the-fly adaptation of the transfer interval based on the feedback of the robot but, instead, it is the interpolator’s task to cope with delayed packets. As a result, the times between two received packets is sometimes lower than 100 ms caused by the delay of the first of these two packets.

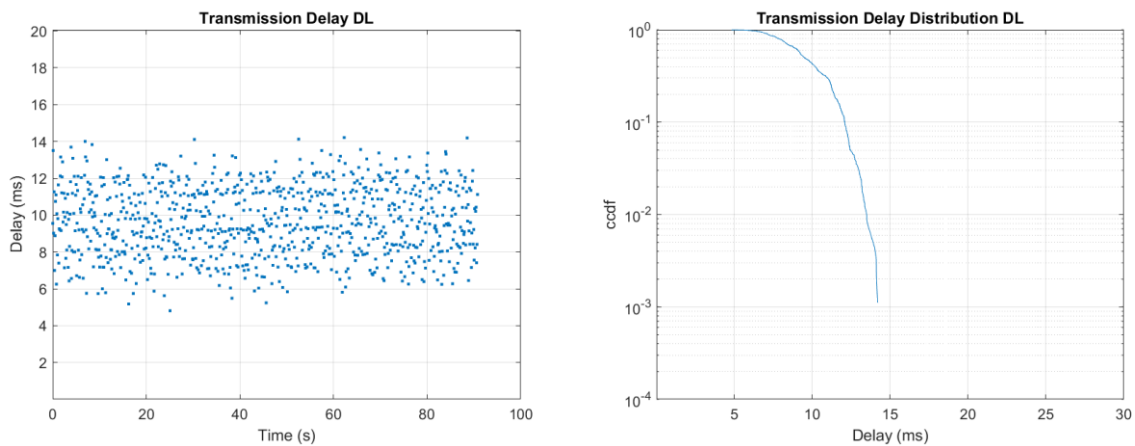


Figure 4-13: DL latency of motion control frames with 20Mbps DL cross-traffic.

When increasing the cross-traffic to 20Mbps, we immediately observe an increase in latency as shown in Figure 4-13. For 99% of the packets, we only achieve a latency of less than 14ms, which is an increase by 40%. Accordingly, the spread of frames on the receiver side becomes larger (Figure 4-14).

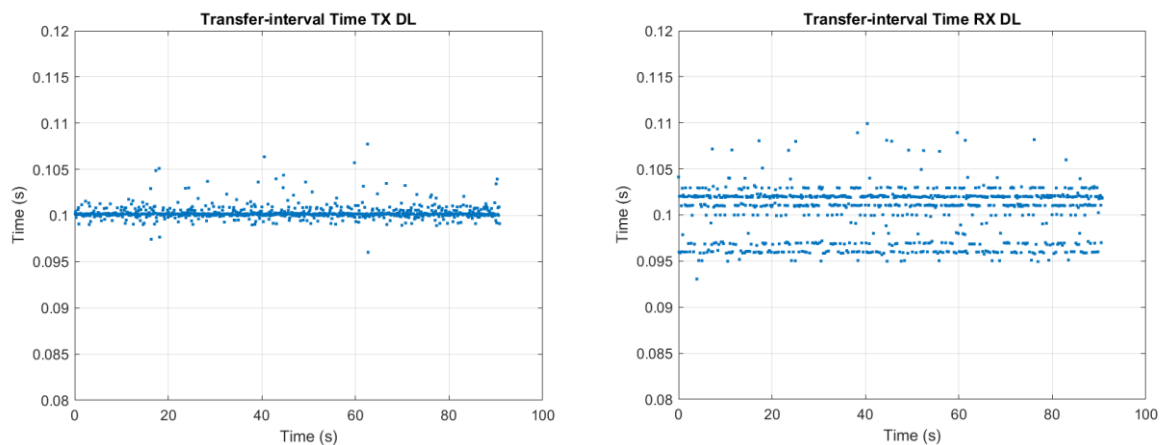


Figure 4-14: Transfer-interval time measured after MA (left) and before MS (right) with 20Mbps DL cross-traffic.

The last test case uses 150 Mbps background traffic, which was close to the limit we were able to transmit error-free during the performance test at the given UE location. Again, latency and jitter increase for the control packets, for 99% of frames we now achieve a less-than-16.5ms latency (Figure 4-15).

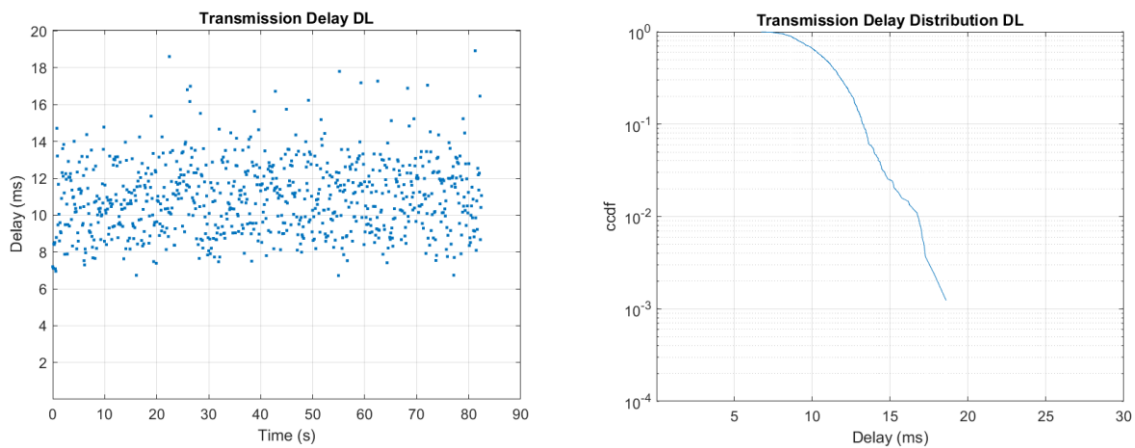


Figure 4-15: DL latency of motion control frames with 150Mbps DL cross-traffic.

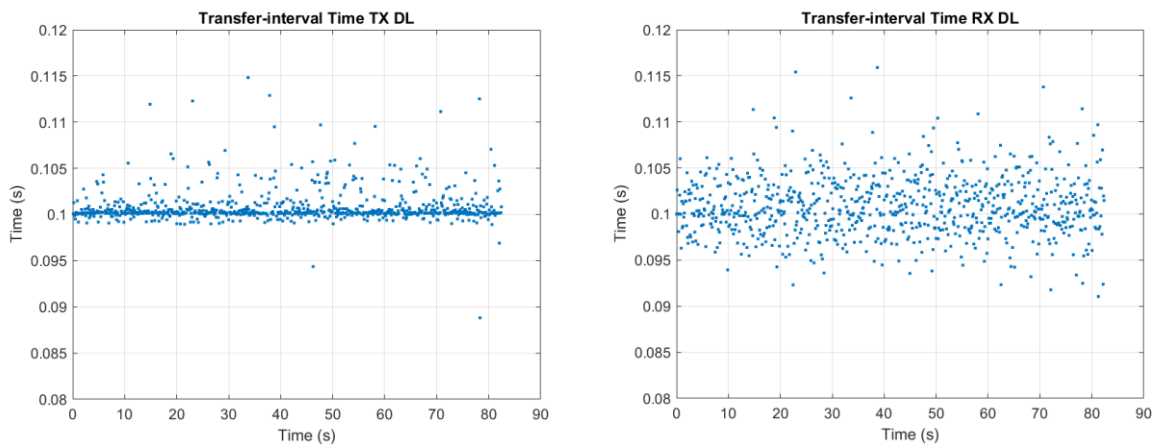


Figure 4-16: Transfer-interval time measured after MA (left) and before MS (right) with 150Mbps DL cross-traffic.

For completeness, we also show the latency in UL in Figure 4-17. As we do not apply cross-traffic in UL, the latency remains similar between the test cases.

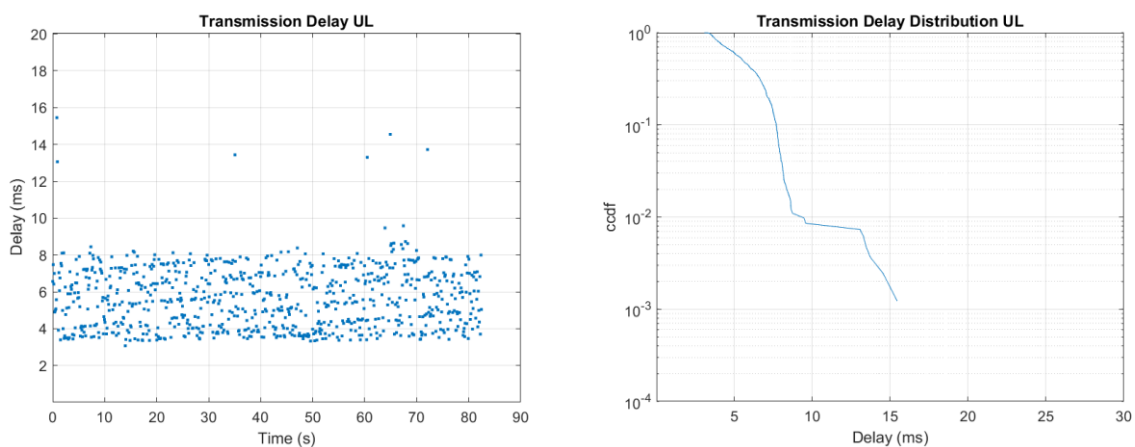


Figure 4-17: UL latency of motion control frames with no UL cross-traffic.

The important measure for the MS to achieve a smooth execution of the trajectory is the jitter. While a constant high latency only results in a delay in execution, the variation in latency can cause uneven interpolation between the requested joint vectors. To compare the jitter of frames when they reach the MS, we derive the deviation from cycle time in Figure 4-18, which is based on the results of Transfer-interval times in Figure 4-12, Figure 4-14, and Figure 4-16.

re 4-16, respectively. The deviation represents the relative difference of the measured transfer-interval and the cycle time of 100ms. Looking again at 99-percentile, we have a deviation of 5%, 7.5%, and 10% from the 100ms cycle time for the 0Mbps, 20Mbps, and 150Mbps test cases, respectively.

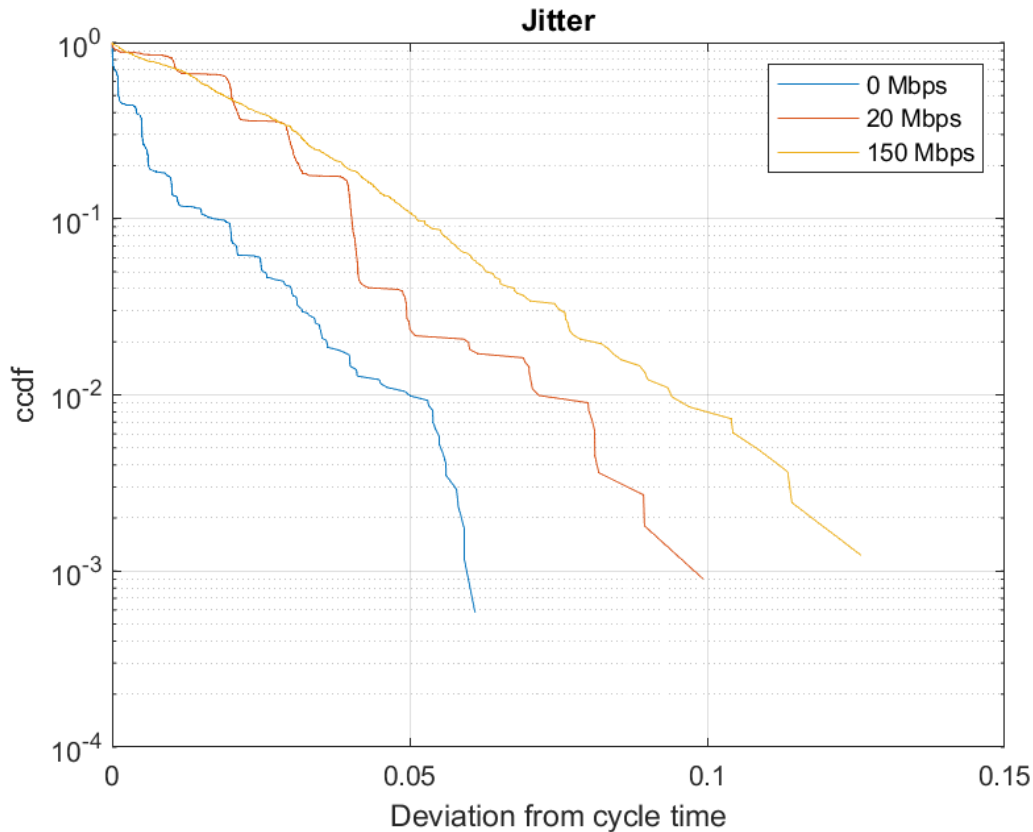


Figure 4-18: Deviation from cycle time of motion control packets with 0, 20, and 150 Mbps DL cross-traffic.

Based on these network results, we further investigate which impact the increase in jitter has on the robot motion. Overall, we observed that under all tested cases the robot motion shows no visible deterioration. The executed trajectory is most of the times without interruptions and motion is smooth. This indicates that the designed interpolation function and split between MS and MA is performing quite well in networks without deterministic latency. Nonetheless, there are some measurable degradations on the robot motion, which leads to a high-frequent change in speed of the individual joint. While not immediately visible, this can lead to inaccurate execution, timing issues when dealing with coordinated tasks and increases stress on the material such as the servo motors of the robot. In general, the location of the robot poses is always very accurate, since the joint values commanded by the MA are not altered. The only variation comes with the timing of the commands, i.e., when is the next command received and executed. Hence, we decided only to investigate the joint speeds of the robot and to compare if the executed and commanded trajectories are moving with the same speed over time. The calculation of the speed based on the trajectory values is explained in Section 4.1.2.2.1.

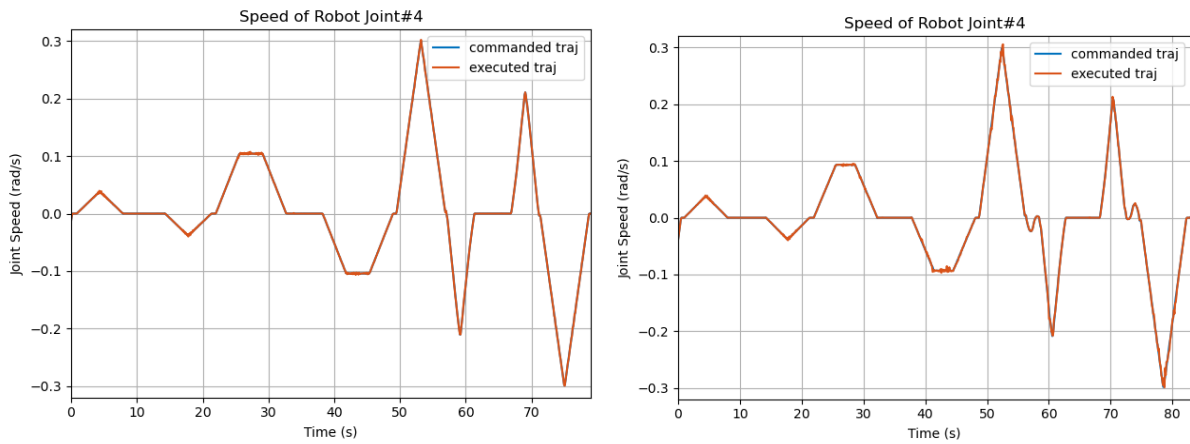


Figure 4-19: Speed of robot joint for 0Mbps (left) and 150Mbps (right) cross-traffic.

Exemplary, we look at joint number 4 of the robot in Figure 4-19, which shows an excerpt from the pickup motion. At first glance, the speed between executed and commanded trajectory seems to be aligned. A closed-up view in Figure 4-20 reveals that the speed deviates from the ideal line, indicating that the acceleration of the robot fluctuates.

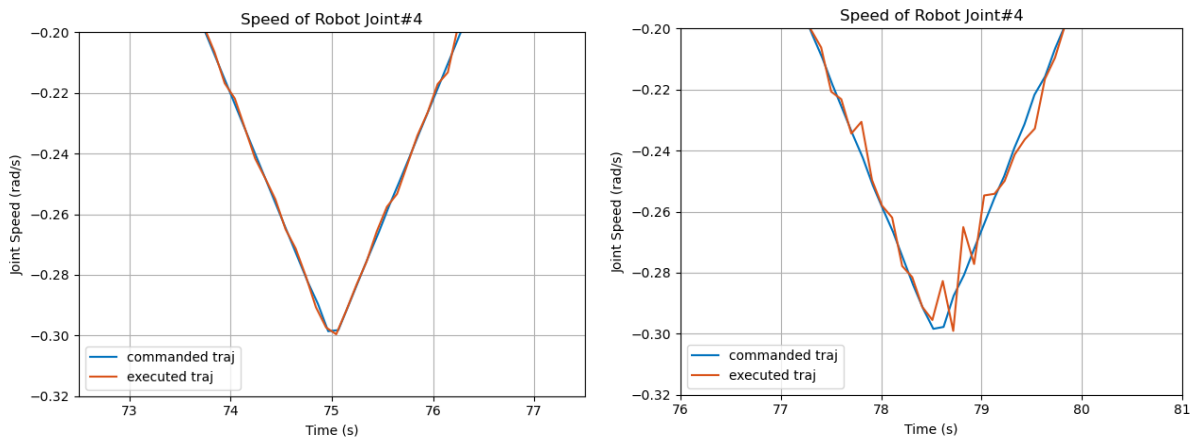


Figure 4-20: Close-up view of speed of robot joint for 0Mbps (left) and 150Mbps (right) cross-traffic.

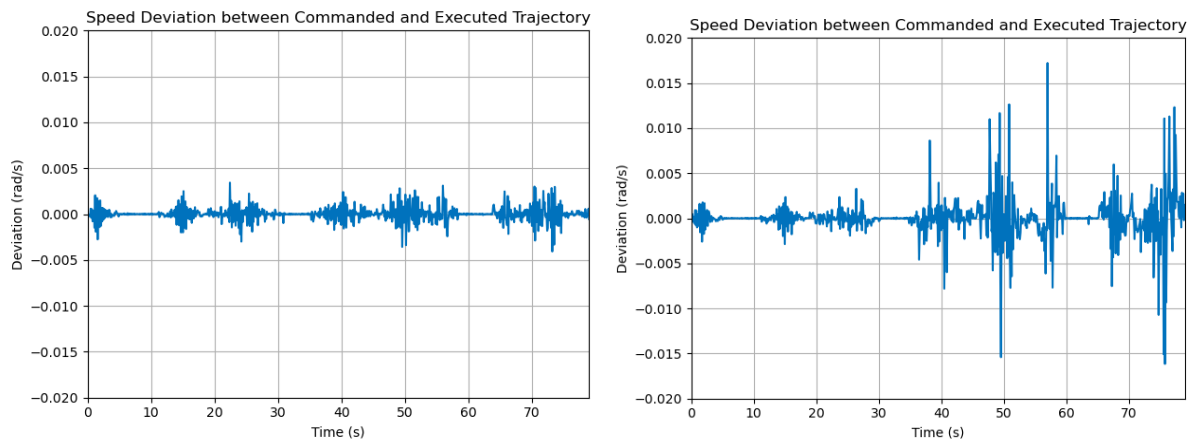


Figure 4-21: Deviation between commanded and executed trajectory speed for 0Mbps (left) and 150Mbps (right) cross-traffic.

We quantified this deviation in Figure 4-21, where we can see a 5-fold increase in the maximum deviation from 0.003 rad/s to 0.015 rad/s in the worst case.

Compared with the initially assumed non-functional requirements of the UC (see [3]), the results suggest the following. We have seen a lower service bitrate (close to 20 kb/s) for the robot control, as the transfer interval was chosen to be 100 ms (instead of 20 ms) for the reason of increasing the robustness of the robot operation against jitter. This was also necessary, as the initially targeted E2E latency of 1–7 ms could not always be achieved by the 5G System, see Figure 4-11, Figure Figure 4-13Figure 4-15Figure 4-17, especially for increased cross-traffic. The increased jitter caused by the cross-traffic induces a deviation between the planned and executed trajectories, despite the ability of the interpolator to smooth out the curves and to keep the robot operational. This deviation becomes critical and visual by the human eye once the jitter exceeds more than 10-15 % of the cycle time, in this case 10-15 ms. In this regard, the robot control offloading concept could successfully be validated given the camera stream data rate is sufficiently low – being the reason that the camera data rate in the experiments was chosen lower as compared to [3].

4.2 Taiwanese Testbed

This section deals with the final integration of 5G with combined UC-1/UC-2 and additional UC [3].

4.2.1 Combined UC-1/UC-2: Process Diagnosis Using Augmented/Virtual Reality with CNC and Sensing Data Collection

4.2.1.1 Wired Performance Evaluation Using Network Emulator

In order to evaluate the impact of various network impairments on the user experience, a test program was designed and documented in [2]. This section extends the description of the applied methodology and is followed by the updated test results.

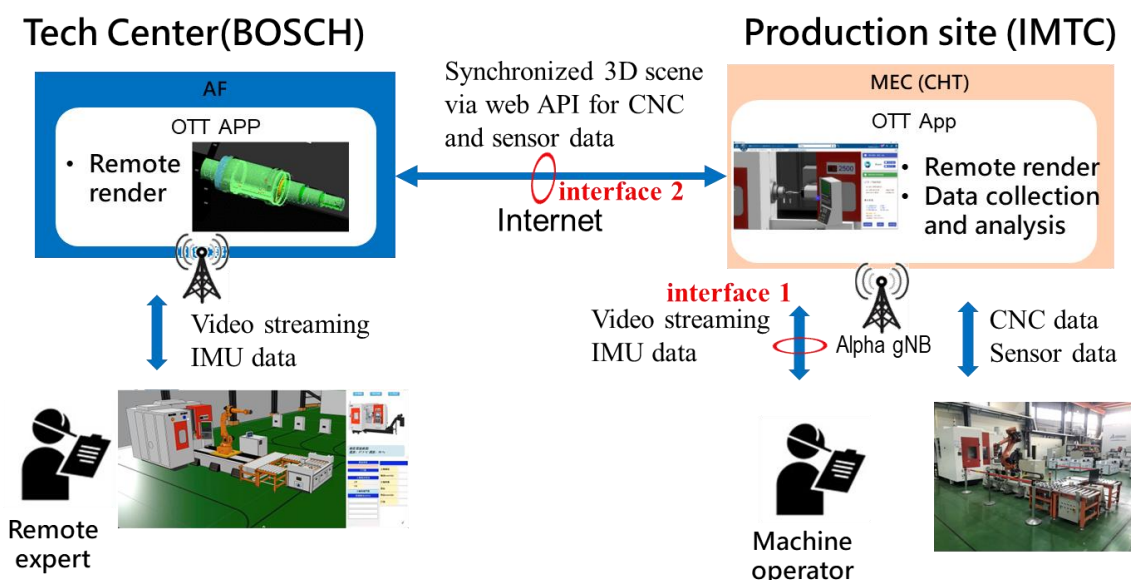


Figure 4-22: Illustration of inter-site use case.

Figure 4-22 shows the simplified architecture of inter-site UC, which is the extension of the combined UC-1/UC-2 and will be further elaborated in Section 4.3. There are two interfaces to be evaluated. Interface 1 is the 5G air interface and is used to transport the video streaming and IMU data between the render server and 5G end devices that the machine operator

is using (e.g., HMD and tablet). In addition, interface 2 is the typical Internet transport network, whose QoS is not guaranteed by the 5G system, and is used to transport CNC and sensor data via web API.

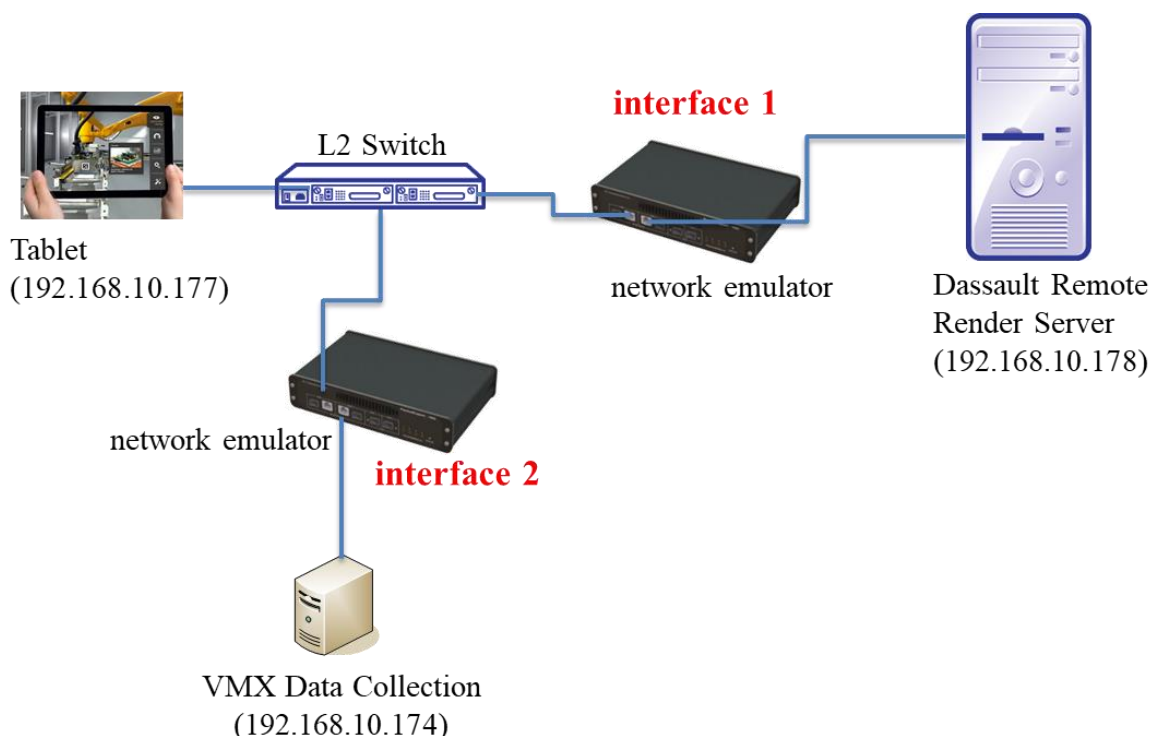


Figure 4-23: Network architecture of impairments emulation.

Figure 4-23 illustrates the corresponding wired architecture of impairments emulations using a network emulator integrated at either interface 1 or interface 2. First, in order to record the baseline performance, the network emulator acts as a simple Ethernet bridge and does not introduce any impairments. The dominant traffic measured at interface 1 is UDP downlink transmission, which carries the downlink streaming video.

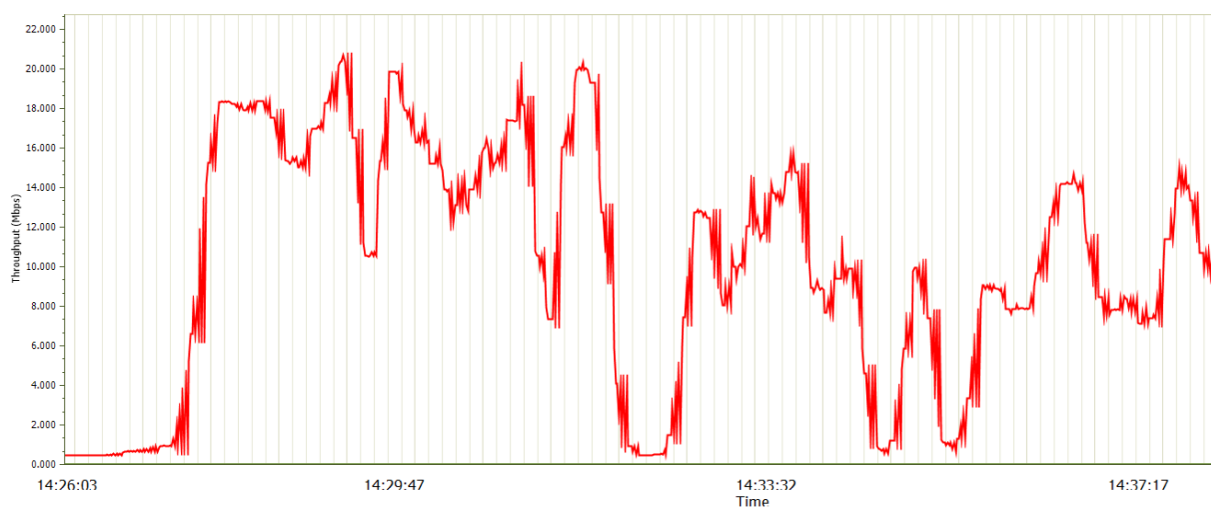


Figure 4-24: Throughput measurements of remote render over ideal transport network.

Figure 4-24 shows the data rate fluctuating between 2 and 22 Mbps according to the speed of the movement of the tablet. It is obvious that the faster one moves the tablet, the higher the throughput measure.



Figure 4-25: Snapshot of streaming video via remote render over ideal transport network.

A snapshot of the streaming video is shown in Figure 4-25 with 30 frames per second and 1920*1080 resolution. If we introduce bandwidth throttling with 10Mbps, the quality of the video is degraded and becomes jerky.

Now, let us consider what happens if we impose simulated latency on interface 1. Table 4-1 describes the impact on the user experience when three uniform distributions are applied. The delayed values vary uniformly between the minimum and maximum values. The visual interaction with the 3D digital twin is not affected when 5~15 ms latency is introduced. The quality of the video on the tablet starts to degrade if the latency is increased to 15~30 ms. Finally, the quality of the video is further degraded and becomes difficult to see clearly if the latency reaches 30~50 ms. Based on the measurements described above, we can conclude that the 5G system shall support 22Mbps downlink transmission per UE and one-way delay below 15ms.

Table 4-1: Remote render with simulated latency.

Test ID	simulated one-way latency	user experience
1	5~15 ms	Good visual interaction with the 3D model
2	15~30 ms	The quality of the video starts to degrade and begin to blur
3	30~50 ms	The quality of the video is further degraded

Regarding interface 2, which is used to transport the digital twin data, the measured data rate varies between 0.1 and 0.2 Mbps, as we expected. Similarly, in order to evaluate the impact of the inter-site latency on the user experience, a network emulator is integrated at interface 2 to emulate the real-world latency. Based on the actual measurements via ping packets transferred between HHI in Germany and ITRI in Taiwan, the network emulator introduces 270 ms on average, meaning a 270-ms delay in the update of the EU digital twin of the real TW equipment. This delay, though, does not decrease the human user's quality of experience, because it corresponds to a transport-network inter-site communication delay, not a 5G on-site delay. As the kinematics of the 3D model is based on the machine data from the VMX data collection server, there is an obvious time shift between the 3D model at two sites.

It should be noted that the remote expert is unaware of the time-shifted 3D model. We can conclude that the inter-site latency does not have strong impacts on the user experience of the remote expert and on-site machine operator. Latency critical scenarios will be demonstrated locally rather than inter-continental.

4.2.1.2 Integration of 5G with Process Diagnosis Using AR/VR

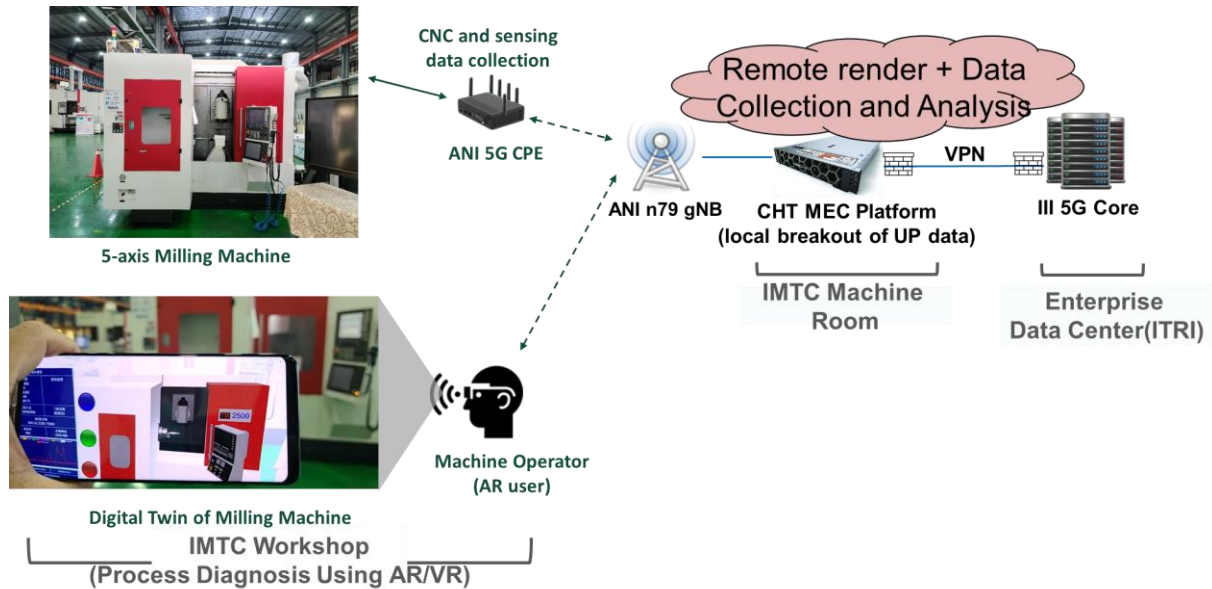


Figure 4-26: Integration of 5G system with combined UC-1 and UC-2.

Figure 4-26 shows the final architecture of the network integration of 5G system with the combined UC-1 and UC-2. Two OTT applications including data collection and analysis and remote render are hosted by the dedicated server, which is connected to the MEC platform for local breakout of user-data streams. A 5G CPE is used to provide wireless connectivity to the milling machine to transport CNC machine and sensing data towards the data collection and analysis. In addition, the remote rendering technique has been used to transport the video stream of rendered scene to the tablet via 5G. The viewport of 3D scene can be updated with the IMU information from the tablet so that a smooth user experience of navigating through the 3D scene can be achieved. A more detailed description of the UC implementation can be found in [5]. The combined UC-1 and UC-2 are extended to the inter-site UC and will be described in Section 4.3.

4.2.2 Additional UC: Cloud-based Controller for Fixture System

4.2.2.1 Integration of 5G with Cloud-based Controller

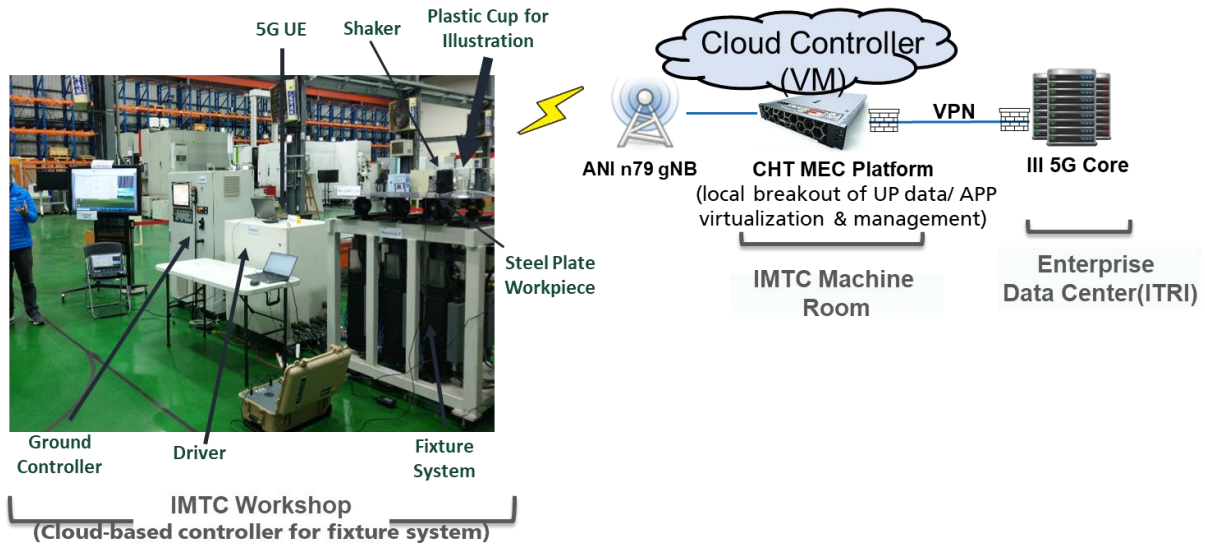


Figure 4-27: Vibration mitigation using cloud-based controller over 5G.

Figure 4-27 illustrates the network integration of 5G with cloud-based controller. Notice that, in addition to the local breakout of user plane data, the cloud controller has been virtualized to the MEC platform so that the OTT application can be managed and monitored. The cloud controller has to send a series of motion commands to the ground controller to reduce the vibration during the milling process in a timely manner via 5G. As the network may not always be able to guarantee the required QoS of the UC due to unpredictable impairments of the wireless channel, two key performance measurements have been monitored, namely: latency and buffer size, to inform the factory personnel about imminent networking issues that could jeopardize the machining process. Latency is used to measure the application processing time and 5G transmission time. Buffer size indicates the motion commands received at the ground controller. If these performance indicators exceed certain thresholds, the factory personnel will be notified to take countermeasures to prevent a further degradation.

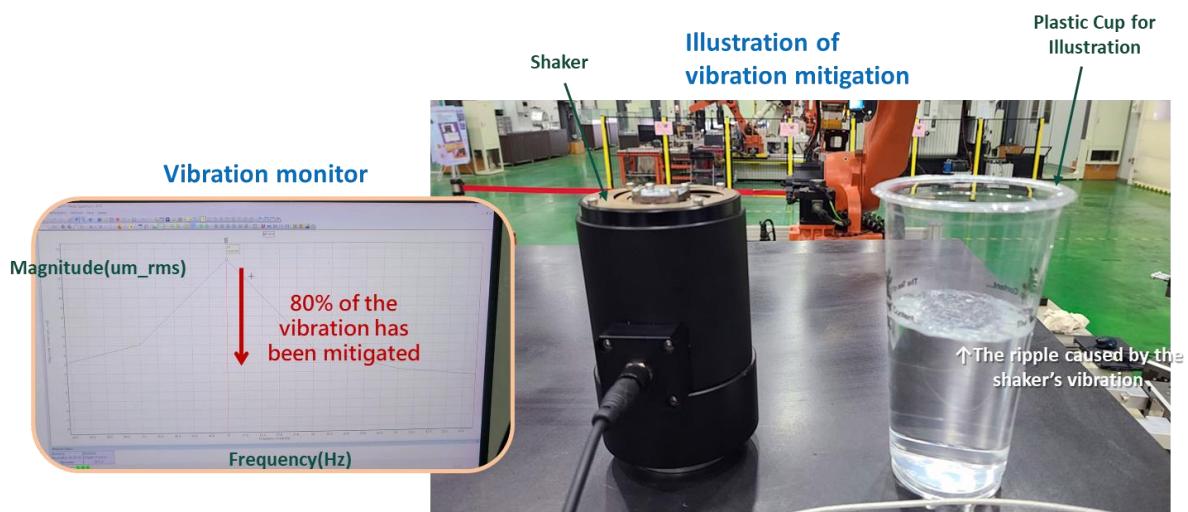


Figure 4-28: Illustration of vibration mitigation.

The details of the monitoring and alerting functions enabled by the MEC platform can be found in [5]. The validation of this UC using 5G is shown in Figure 4-28, where a plastic cup is used for illustration. The objective is to suppress the vibration introduced by a shaker with frequency under 500 Hz. The test results show that 80% of the vibration has been mitigated in terms of magnitude.

4.3 End-to-end Testbed

This section is dedicated to the UC deployed across the intercontinental setup.

4.3.1 Inter-site UC: Remote Expert Support for Process Diagnosis, Extension of UC-2 by Exchanging Data Across the Two Continental Sites

Here, we present our intercontinental use case which extends UC-2 by enabling remote expert support for process diagnosis through data exchange across our test sites in EU and TW. For this intercontinental use case, we have considered test scenarios including *remote commissioning of machines* (IS-4) and *remote expert support for process diagnosis* (IS-5) [4]. Our objective is to establish a synchronized digital twin system across the two sites, facilitating real-time expert support and machine diagnostics remotely. This intercontinental use case builds upon the similar use case deployed in TW. Please note that all testing activities reported in WP5 deliverables and related to the TW deployment of UC-2 and its technological components are considered preliminary and functional for the intercontinental use case as well. Once the fundamental network requirements and architectural tests were completed successfully in the TW use case, the primary focus for this intercontinental use case was to validate the feasibility of the scenarios at an application level. Hence, further validation tests have not been necessary at the 5G networking level. By integrating these systems, we aim to enhance the capabilities of remote machine diagnosis, adjustment, and in-depth analysis of process errors.

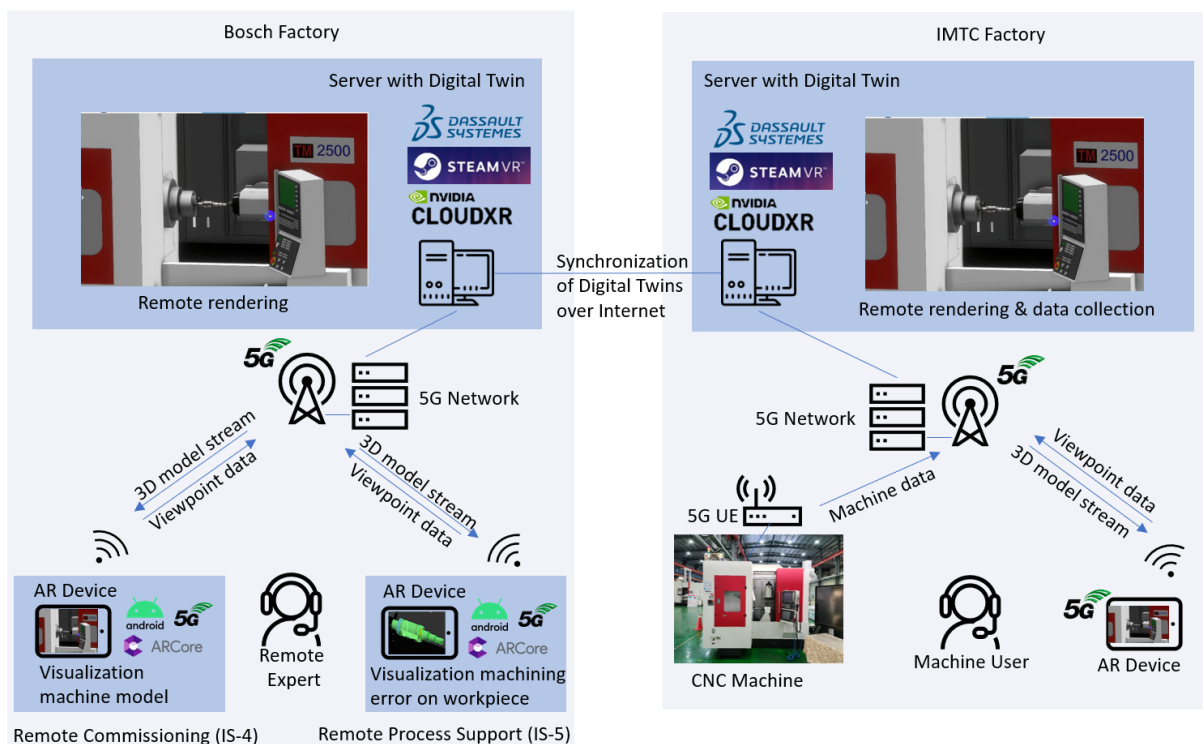


Figure 4-29: Architecture of the inter-site use case.

The E2E testbed is an integration of both testbeds deployed at BOSCH and ITRI, respectively. The purpose of the E2E testbed is to enable collaborative UCs requiring coordination across both sites. The corresponding architecture of the testbed is described in Figure 4-29.

The BOSCH side is an extension of the TW setup shown in Section 4.2. On both locations, an identical copy of the remote rendering server for creating the digital twin has been deployed. Both use the same Dassault Systèmes software for the 3D machine model and SteamVR in combination with CloudXR for the remote rendering and streaming to the end device. In order to synchronize both digital twins, a WebAPI was implemented for data collection from machine tool in IMTC's demo site. Dashboards implemented in Node.js and shown in 3D scene are used to expose in real-time the sensor data from the physical machine on the TW site. The synchronization between the two digital twins happens on the following three data sets:

1. Production management information: current work order for the workpiece and progress of machining process.
2. Machine Operational Data: machine coordinate, spindle speed, federate, spindle loading.
3. Sensing Data: 3-axis vibration data from spindle and workpiece, totally 6 channels of sensing data.

With the infrastructure that we have set up, as described above, we can facilitate two inter-site use case scenarios, IS-4 and IS-5 [4]. In these use cases, the expert on the BOSCH site uses an AR device, in our case a mobile phone or tablet, to visualize a remote machine deployed at the IMTC site. The expert can then support the user in the TW factory to commission and/or maintain the entire machine (IS-4) or perform in-depth analysis of a workpiece in case of process errors (IS-5).

Besides the end-to-end functional tests of the digital twin synchronization between the sites, we additionally provide in the next section test results on EU site end-devices. Since the EU site uses a different 5G deployment and smartphones/tablets than the TW site, some application test cases of the digital twin visualization are presented to validate the performance.

4.3.2 End Devices on BOSCH's Side

The visualization and augmentation of the machines 3D model is done on two Android devices. The two key requirements for the end device are the 5G support for private networks and the support of Googles AR core application which is used for the visualization.

We successfully tested the application with the smartphone Asus Zenfone 8 which met both the requirements (Figure 4-30).

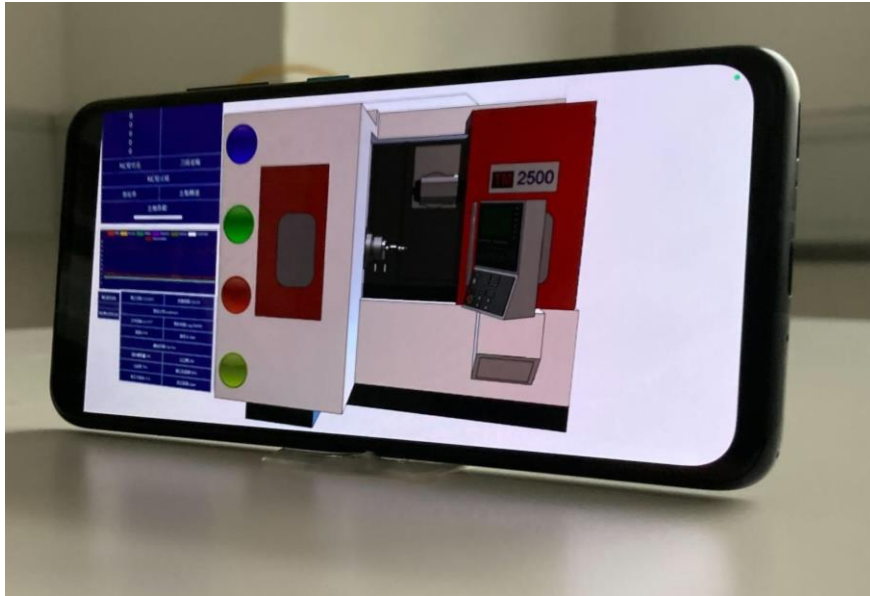


Figure 4-30: Virtual machine on 5G smartphone.

We employed a workaround using an external 5G Quectel module in combination with a Raspberry Pi to bridge the 5G connection to the tablet (Figure 4-31). This introduces a small additional forwarding delay. We measured a bridging delay below 1 ms, which is barely noticeable considering the longer network delay as investigated in the following.

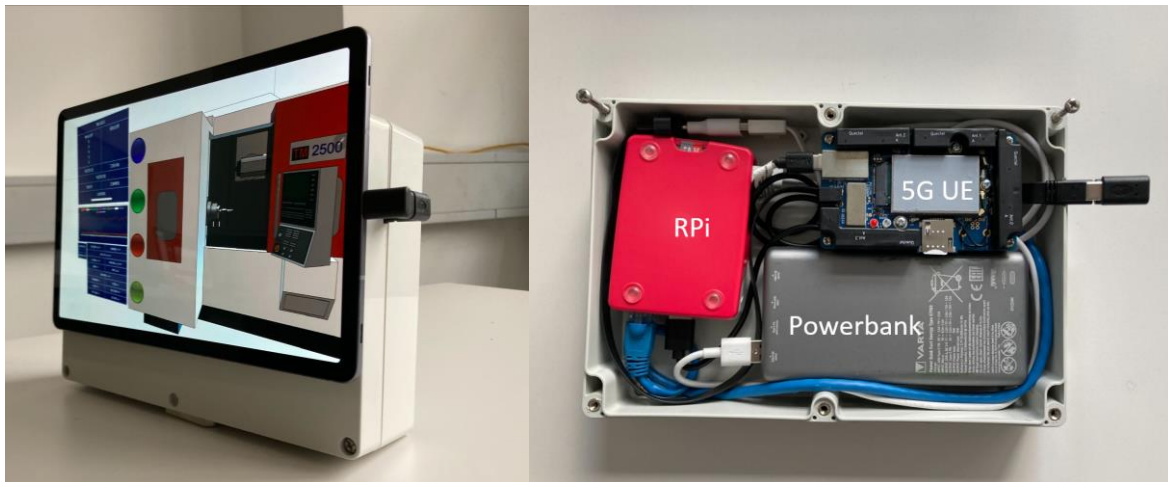


Figure 4-31: Virtual machine on tablet (left) with external 5G module (right).

We conducted some performance measurements with the end devices to capture the application characteristics and evaluate the network performance. We applied the same method using synchronized network taps as described in Section 4.1.

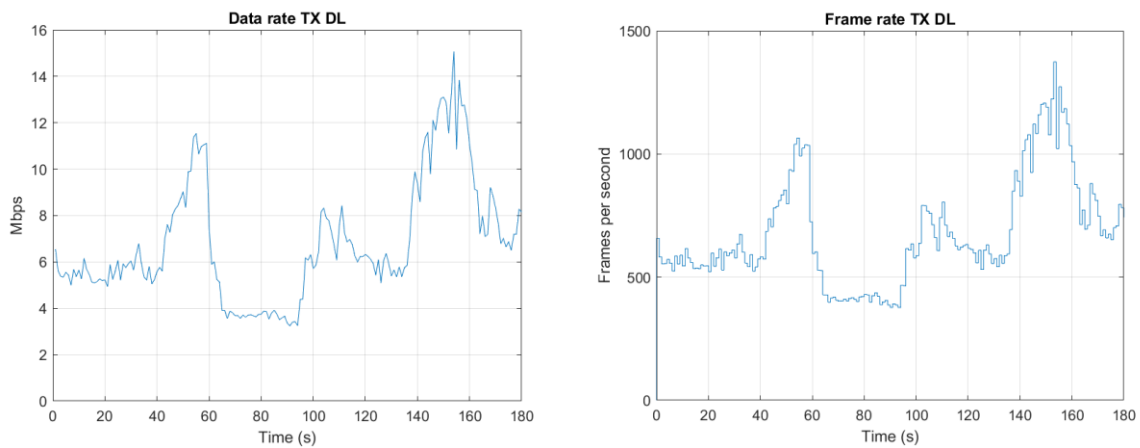


Figure 4-32: Downlink traffic for machine visualization as data rate (left) and frame rate (right).

Since all the machine data is rendered on the server and only the current scene is streamed directly to the device, the traffic is mostly in downlink. In Figure 4-32, the downlink data rate and frame rate are shown. The frame rate fluctuates depending on the speed of the movement. If the viewpoint does not change, the video stream remains static and hence data rate requirements are lower. We measured minimum 4 Mbps and a maximum of 15 Mbps. The results are in line with the emulation results conducted in Section 4.2. There, even higher data rate above 20 Mbps has been measured. With additional headroom around 25 Mbps should be expected for this application in DL.

In uplink, only the viewpoint of the device is reported to the server, such that the correct scene can be rendered and streamed back to the user. The rate is hence more consistent and lower compared to DL with around 1 Mbps (Figure 4-33).

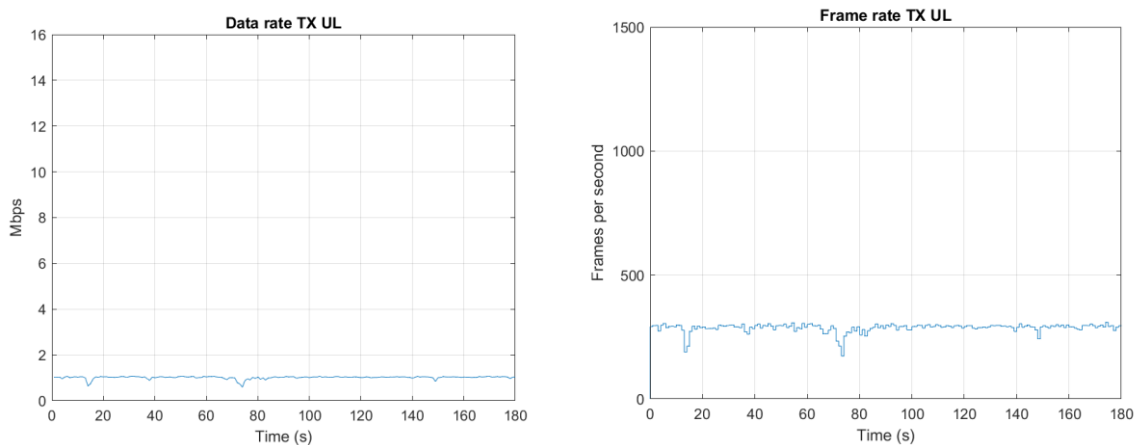


Figure 4-33: Uplink traffic for updating viewpoint as data rate (left) and frame rate (right).

The latency distribution as CCDF is shown in Figure 4-34. Comparing the 99.9% value, we see that DL latency is < 15 ms, while in UL the latency is approximately twice as high with less than 30 ms. In Section 4.2, several ranges for one-way latency have been tested and evaluated. Based on this result we can conclude that the DL latency is low enough to achieve a consistently good visual interaction on the device. The critical path appears to be UL direction which reaches up to 30ms, where some video quality degradation has been observed in the emulated study. Overall, the tested user experience in terms of responsiveness to the scene changes was good with only minimal interruption in the video during faster movements, which lead to higher data rate and furthermore slightly higher latency.

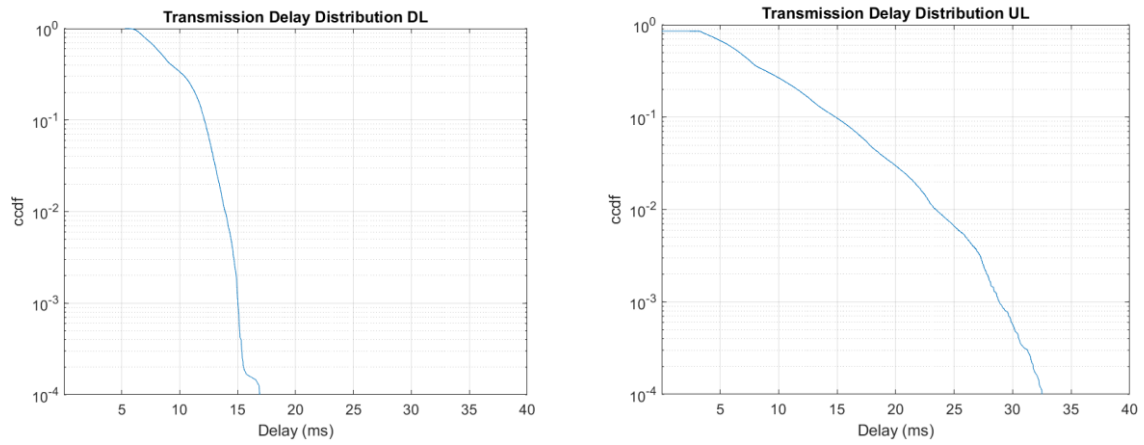


Figure 4-34: Latency distribution for downlink (left) and uplink traffic (right).

5 Conclusions

WP5, “Integration, Demonstration & Verification,” aimed to unify in a unique intercontinental testbed the network and application components developed in WP4, matching the E2E system designed in WP2, taking into account the roles and capabilities of all the players involved in private 5G networks for the smart industry, and considering the outcomes of WP3. [1] and [2] were dedicated to the initial and intermediate planning of the operations leading to such a use-case-based multi-site system, and they reported on the in-lab and preliminary cross-testbed integration and testing activities carried out until March 2022. Building upon these results, the present deliverable concludes the reporting of activities related to WP5, covering the full implementation of the 5G network supporting the UCs and the collection of experimental results from the execution of such UCs. In particular, we provided all remaining technical and implementation details on the local and E2E connectivity aspects compared to what reported in [1] and [2]. We elaborated on the features of the advanced applications and devices involved in the project’s UCs, and we reported the experimental results and KPI measurements collected from the testbeds.

The activities related to UC-3 “Robot Platform with Edge Intelligence and Control” resulted in a very helpful testbed framework and platform for 5G performance evaluation. More concretely, performance cannot only be measured in terms of network latency but with respect to actual manufacturing process KPIs, such as the accuracy of robot trajectories as a function of the network latency or jitter. Under most test cases, the robot motion shows no visible deterioration; however, some measurable degradations on the robot motion can be detected (up to a five-fold increase in the worst case for high cross-traffic), leading to a high-frequency change in speed for the individual joint. While not immediately visible for low cross-traffic, this can lead to inaccurate execution, timing issues when dealing with coordinated tasks and increases stress on the material such as the servo motors of the robot. These results suggest that a proper motion application design can principally cope with non-ideal latency and jitter in a private 5G setting, but lower jitter compared to what was measured in the experiments, especially in presence of significant cross-traffic, is generally desired. Apart from this, making explicit use of edge compute functionalities with multiple applications (robotic control, computer visions from camera images) demonstrate well the importance of edge compute along with (integrated with) 5G functionality. It is anticipated that this would lead to improvements of the overall equipment efficiency of plants if rolled out in the future. In addition, the evaluations showed that private 5G networks are capable to enable novel industrial use cases that have the potential to make manufacturing more efficient. Of particular importance to BOSCH as an end user, was the understanding of the operation and maintenance of private 5G networks. UC-3’s results provided an excellent understanding on 5G particularities on robotic use cases, the impact on corresponding product concepts, and with this on new business opportunities in the context of 5G-enabled factories. We successfully demonstrated how an intelligent motion control design can cope with non-ideal networks, nonetheless predictable and guaranteed network performance remains a key feature for many manufacturing applications. Of great interest to BOSCH are Time-Sensitive Networking (TSN) and Ultra-reliable and Low-Latency (URLLC) features in 5G that were not commercially available during the project phase. In future, BOSCH will continue its innovation and research work on such advanced and beyond 5G features, for which the insights and results of the 5G CONNI project laid an important foundation.

Moreover, from the implementation of UC-1, UC-2, and the additional and cross-site UCs, we noticed that using 5G private network as Internet-of-Things backbone for machine operational and sensor data collection can achieve higher sampling rate and higher data flow rate so that more process features can be extracted from machining process. Therefore, we can do

more sophisticated analysis in the edge computing platform. Process diagnosis using augmented reality can also benefit from higher data rate and low latency of private 5G network. High fidelity 3D models can be deployed in the edge computing platform equipped with high performance graphical cards and render the 3D scene and send to end user devices in terms of video streaming to provide more simulated results from the machining process and speed up the process diagnosis at remote sites.

Globally, with the deployment of its testbeds and the execution of its use cases, 5G CONNI has contributed to demonstrating in representative scenarios how 5G technologies will reshape the industrial world and its manufacturing processes, leading to higher efficiency and reduced operational costs for companies. Further, the concrete test and validation results obtained with 5G CONNI's experiments and the possibility of each partner to get to know the other partners' business requirements and technical competencies, have convinced the consortium that private 5G networks have the potential to be widely adopted and extensively deployed in industrial scenarios. Partners hosting WP5 testbeds have learned that a 5G network can be entirely managed and operated by the IT department of a private company; 5G component vendors have been able to work on solutions that fit such private entities' requirements; and academic partners have been able to gather useful data and information from experimentation and setting the foundation for future research in the telecommunication field. Because of this, the consortium considers that the project has been successful in its activities and has achieved relevant goals.

It is important to conclude with another meaningful learned lesson: private standalone 5G networks are already a reality and de facto commercially available, but the extensive adoption of full-fledged 5G networks for private use will still require a few years, especially to substantially differentiate itself from certain existing 4G-based telecommunication solutions. During 5G CONNI's activities, we have experienced that 5G is partially not capable to exploit widely and in real life its promised technological potential yet, including that of some innovations investigated in 5G CONNI's WP3 and WP4 themselves and prototyped in WP5. Examples of available features and solutions validated by the project and ready to market include the enablement of edge computing via traffic localization and the deployability of 5G network functions in flexible architectures across different sites and over different virtualization environments (as in WP5's testbeds), with a management system that allows for smooth operations and simplified control over the network resources. At the same time, for instance, existing commercial UEs, base stations, and 5GC are still not entirely supporting (or at least not in complete end-to-end chains) features like TSN, URLLC, machine-type communications, certain millimeter-wave radio signals, and other advanced components described in or being part of 3GPP standards. In conclusion, private 5G networks still have some way to go before showing their fullest potential. Yet, this will happen undoubtedly, and it will become common practice for common businesses to have their own 5G, changing the mobile network ecosystem from being populated only by nation-wide public networks to hosting a plurality of "small" private customized networks.

6 References

- [1] 5G CONNI, "[E2E in-lab system integration report](#)," D5.1 report, WP5, June 2021.
- [2] 5G CONNI, "[E2E In-Factory System Integration Report](#)," D5.2 report, WP5, March 2022.
- [3] 5G CONNI, "[Report on use cases & requirements](#)," D1.1 report, WP1, July 2020.
- [4] 5G CONNI, "[Final report on private 5G network architecture and operator models](#)," D2.2 report, WP2, September 2021.
- [5] 5G CONNI, "Specification and implementation of advanced functionalities," D4.3 report, WP4, September 2022.
- [6] M. Lind, "Real-time quintic Hermite interpolation for robot trajectory execution," *PeerJ computer science*, p. 13, 2020.
- [7] 5G CONNI, "[Intermediate report on private 5G network architecture](#)," D2.1 report, WP2, September 2020.
- [8] 3GPP, "[System architecture for the 5G System \(5GS\)](#)," Technical Specification 23.501, Rel. 16.